Datum
2024-02-28

Dnr
2021-015905

Projektnr
52415-1

Energimyndighetens titel på projektet – svenska E-THRUST - Design Optimering av Hybridelektriska och Vätgasdrivna Flygplan
Energimyndighetens titel på projektet – engelska E-THRUST - Design Optimization of Hybrid-Electric and Hydrogen-Powered Aircraft

Universitet/högskola/företag	Avdelning/institution
Mälardalen University	Future Energy Center

Adress Universitetsplan 1, 722 20 Västerås, Sweden
Namn på projektledare Prof. Konstantinos Kyprianidis
Namn på ev övriga projektdeltagare Mr. Dimitrios Bermperis, Mr. Kreshnik Margaritari, Mr. Mavroudis Kavvalos, Ms. Mathilda Cederblad, Dr. Stavros Vouros, Dr. Avinash Renuke, Mr. Jim Cleasson, Dr. Michael Sielemann, Mr. Mikael Stenfelt, Mr. Michael Säterskog
Nyckelord: 5-7 st Hybrid-Electric, H2, Gas Turbines, Optimisation, Infrastructure

Forward

The E-THRUST project is an integrated collaborative project bringing partners together across Sweden. It is funded by Energimyndigheten (Swedish Energy Agency) under the Fossilfritt flyg 2045 programme *"Elflyg och Flyg med vätgasdrift inkl. tanknings- och laddinfrastruktur"*.

The project has been led by Prof. Konstantinos Kyprianidis at Mälardalen University (MDU), The report reported herein, has been carried out at the Future Energy Center at MDU in Västerås, Sweden.

The integrated MDU team included: Mr. Dimitrios Bermperis, Mr. Kreshnik Margaritari, Mr. Mavroudis Kavvalos, Ms. Mathilda Cederblad, Dr. Stavros Vouros, and Dr. Avinash Renuke. Saab (Mr. Mikael Stenfelt, Mr. Michael Säterskog) and Modelon (Mr. Jim Cleasson, Dr. Michael Sielemann), are acknowledged for their co-financing and contributions that have enabled this work.

Table of Contents

Box 310 • 631 04 Eskilstuna
Telefon 016-544 20 00 • Telefax 016-544 20 99
registrator@energimyndigheten.se
www.energimyndigheten.se
Org.nr 202100-5000

Sammanfattning

Elektrifiering av flygplansframdrivning har stor potential för att minska flygets miljöpåverkan. Serie/parallell partiell hybridarkitektur väljs och utforskas i ett litet pendlingsflygplan med 19 passagerare för 2035 teknologi nivå. Ett multidisciplinärt ramverk utvecklas och används för representation av individuella framdrivningssystem, flygplan och uppdragsbedömning. Trots den ökade designflexibiliteten hos den elektriska hybridkonfigurationen undergräver det extra batteriet avsevärt fördelarna med bränsleförbrukningen som uppnås genom hybridisering. Ändå avslöjas flera designsynergier och avvägningar mellan designen av de termiska och elektriska kraftverken. Dessutom framhävs avancerade energihanteringsstrategier genom hela uppdraget i syfte att dra nytta av den installerade elektriska energin så mycket som möjligt.

Vätgas är en annan möjlig lösning för att mildra flygets miljöpåverkan. Direkt väteförbränning på ett turboprop 19 passagerarflygplan utforskas genom det multidisciplinära framdrivnings- och flygplansbedömningsverktyget. Vätgasförbränning möjliggör en stor minskning av bränsleförbrukningen på grund av bränslets energitäthet. Låg mognadsnivå för kryogena lagringstankar och termiskt konditioneringssystem resulterar dock i ökad flygplansmassa. Sammantaget förbättrar vätgasutnyttjandet motorns prestanda men den extra vikten uppväger alla fördelar för den totala energiförbrukningen jämfört med ett konventionellt Jet-A-brinnande flygplan med samma teknikniv̊a. Trots det är CO2-utsläppen från de vätgasförbrännande flygplanen noll, vilket helt förnekar den negativa miljöpåverkan från dagens flygplan.

Kraven på markinfrastruktur bedöms utifrån möjliggörande av elektrifierat och vätgasdrivet flyg. En systemmodell för ett energinav utvecklas med egen el- och väteproduktion, lagring i batterier, komprimerade och flytande vätgastankar samt bilateralt utbyte av el och väte med det nationella elnätet. En flygplatsnav av denna layout ska inte fungera i öläge utan snarare i anslutning till nätet: när elpriset är tillräckligt lågt ska egen produktion av el och vätgas användas för att driva flygplanet och markkonsumenten på flygplatsen. Samtidigt ska flygplatsen fortsätta att använda extern försörjning från el- och vätgasnäten när det är ekonomiskt och miljömässigt hållbart. Slutligen ska flygplatsnavet stödja elnätet genom att sälja el och vätgas vid tider med överskott.

Sammantaget kan en tät koppling och samproduktion mellan energinätet, flygplatsen och flygplanet vara möjligören för övergången till fossilfri flygning inom ett hållbart energiekosystem.

Summary

Electrification of aircraft propulsion holds great potential to reduce the environmental impact of aviation. The series/parallel partial hybrid architecture is selected and explored in a 19 passenger small commuter aircraft for 2035 assumed technology level. A multi-disciplinary framework is developed and used for the representation of individual propulsion systems, aircraft, and mission assessment. Despite the increased design flexibility of the hybrid electric configuration the added battery significantly undermines the fuel consumption benefits achieved by hybridization. Nevertheless, several design synergies and trade-offs between the design of the thermal and electrical powerplants are

revealed. Moreover, advanced power management strategies throughout the mission envelope are highlighted with the purpose of capitalizing on the installed electrical energy as much as possible.

Hydrogen is another possible solution for the mitigation of aviation's environmental impact. Direct hydrogen combustion on a turboprop 19 passenger commuter aircraft is explored through the multi-disciplinary propulsion and aircraft assessment tool. Hydrogen combustion allows for great fuel consumption decrease due to the energy density of the fuel. However, low maturity level of cryogenic storage tanks and thermal conditioning system results in increased aircraft mass. Overall, hydrogen utilization improves engine performance but the added weight off-sets any benefits for the total energy consumption compared to a conventional Jet-A burning aircraft of the same technology level. Nevertheless, CO2 emissions of the hydrogen burning aircraft are zero completely negating the adverse environmental impact of today's aircraft.

Ground infrastructure requirements are assessed on the basis of enabling electrified and hydrogen-powered aviation. A system model for an energy hub is developed featuring own electricity and hydrogen production, storage in batteries, compressed and liquid hydrogen tanks, as well as bilateral exchange of electricity and hydrogen with the national power grid. An airport hub of this layout shall not operate in island mode but rather in connection to the grid: when electricity price is low enough, own production of electricity and hydrogen shall be used to power the aircraft and ground consumer in the airport. Concurrently, the airport shall continue using external supply from the electricity and hydrogen grids when this is economically and environmentally sustainable. Finally, the airport hub shall be supporting the power grid through selling electricity and hydrogen at times of surplus.

Overall, a tight connection and co-production between the energy grid, the airport and the aircraft can be the enabler for the transition to fossil-free flight within a sustainable energy ecosystem.

Introduction/Background

The de-carbonization of flight is a major requirement in order to achieve the target of 75% reduction in Landing and Take-Off (LTO) NOx emissions and 70% reduction in fuel burn set by the International Air Transport Association (IATA) [IATA, 2019], which has been set on the back of earlier studies [Krein et al., 2012]. Additionally, aircraft operators are increasingly aiming at direct operating cost reduction, whilst concurrently looking at expanding the flight envelope and increasing versatility and flexibility of aircraft power systems.

Responding to this demand, aircraft manufacturers, as well as the research community have initiated radical designs involving electrification and hydrogen power sources for the future fleet. Direct combustion of hydrogen into the gas turbines promises a 50% reduction in climate impact during flight, whilst fuel-cell propulsion can reach up to 75-90% reductions [Clean Sky 2 JU, 2020]. The previous numbers are configuration- and operation-dependent and require a vast set technological advancement related to: hydrogen storage capacity, fuel cell efficiency, hydrogen combustion system stability, and treatment of pollutant emissions and noise. Furthermore, the associated economic operational overhead needs to be reduced. The associated implementation challenges are well known; however rarely looked from a system-level perspective. A set of emerging scientific needs can be frame, including the following:

- Advanced modelling of aircraft power and propulsion components including gas turbines, electric power systems, energy storage, hydrogen combustion, fuel cells and cooling.
- Integration of individual modules into multi-disciplinary computational platforms for the holistic design space exploration of novel aircraft architectures.
- Optimization of combined hybrid-electric and hydrogen-powered aircraft design and energy management towards efficient operation, improved performance and environmental impact.
- Analysis of needs and potential solutions for energy conversion and distribution infrastructure with consideration of regional challenges and market opportunities.

Hence, evaluation of the novel engine/aircraft configurations requires a system-level approach based on multi-disciplinary and robust computational tools. The potential impact of electrified aviation in regional aviation is represented by a 20% reduction in block fuel consumption, without accounting for life-cycle energy production requirements [Pornet et al., 2014]. Similarly, weight penalties eliminate performance improvements of turbo-electric aircraft featuring a boundary layer ingesting propulsor at the fuselage aft-end [Giannakakis et al., 2019]. More conservative boosted concepts provide operability improvements, albeit without significant fuel saving with 2035 technology levels for all electrical components [Zhao et al., 2019]. In terms of direct operating cost, 6-14% reductions have been estimated for a 150-pax high-span hybrid electric aircraft relative to a non-electrified reference [Bradley et al., 2015]. Nevertheless, these benefits are outperformed when costs associated with increased aircraft weight and complexity are included. Battery re-charging during descent, combined with an optimized energy management system can reduce the overall energy requirement on board [Vouros et al., 2020].

Hydrogen-powered and hybrid-electric aviation has demonstrated directions towards achieving industrial needs in terms of fuel efficiency and potential operational flexibility [Jansen et al., 2017; DelRosario, 2014]. However, it is estimated that operational costs can rise up to 10% per passenger for commuter and regional aircraft, and up to 50% for long-range aircraft, compared to conventional propulsion technologies [Clean Sky 2 JU, 2020]. Hydrogen-fueled long-range aircraft designs based on the traditional tube-and-wing configuration present an 11% reduction in energy utilization on-board [Verstraete, 2013]. However, hydrogen storage and the design of cryogenic fuel tanks requires a balanced compromise between mechanical and thermal requirements [Verstraete et al., 2010]. Novel, blended-wing-body configurations feature improved lift-to-drag ratios and allow better flexibility in the installation and distribution of hydrogen tanks along the aircraft. That yields improved fuel efficiency and mitigated ground noise impact [Guynn, 2004]. Small-scale demonstrators of fuel-cell powered aircraft have revealed the feasibility aspects of this technology [Bradley et al., 2007; Kim et al., 2012]. Nevertheless, further research is required for larger scale demonstrations and for the quantification of environmental impact at transportation network level [Yilmaz et al., 2012]. Further to technological advancements, optimal energy management on board is a driving factor for the efficient utilization of the novel technologies [Bradley et al., 2009].

This short state-of-the-art analysis of novel systems for flight decarbonization demonstrates a wide range of benefits related to installation of hydrogen and electric power sources and storage on board. However, the associated improvements and limitations are often looked individually or through employing simplified modelling approaches which are unable to capture the inter-disciplinary design trade-offs. A holistic system-level exploration is needed looking at the potential capabilities and limitations of such electrification technologies, aircraft architectures and even infrastructure. Based on the future aircraft propulsion configurations and requirements, a radical re-design and integration of energy conversion must be realized. Charging batteries in-between flights requires significant power availability, which should be preferably produced locally to avoid excessive burden on the grid. Hydrogen should be also preferably produced locally, in absence of a well-structured hydrogen infrastructure including transportation and storage. Hydrogen production from electrolysis is one of the preferred routes because of the achieved purity and the exploitation of renewable energy sources, but it is not an economical solution to sustain the consistent power demand. Hydrogen production from biomass gasification represents a more economical solution, followed by fuel upgrading or membrane separation. Local gasification and hydrogen production integrated with high temperature fuel cells that tolerate CO and CH4 can exploit biomass available in the vicinity of the airport and supply the energy needed for charging airplanes batteries, starting up conventional and hydrogen-powered gas turbine engines, and all the other services and requirements that exist in the airport.

E-THRUST, focuses on answering these questions for regional engine/aircraft configurations (up to 19-pax) that are suitable within the Swedish and Scandinavian context and offer zero in-flight carbon emissions. This includes solutions that can burn H2 directly in a turbofan and turboprop configurations, as well as solutions that use fuel cells to covert H2 to electricity that is then used to drive an electrical power system; battery-driven all-electric configurations for shorter ranges are also to be assessed. Regional requirements for airport-level infrastructure, including storage and integration with possible

solutions for local H2 production and electricity generation are be investigated. A dedicated scientific approach is developed to address the research questions set, building on the already established trans-disciplinary expertise within Mälardalen University (MDU). Overall, the project provides a holistic system-level exploration of the potential capabilities and limitations of combined hybrid-electric and hydrogen-powered aircraft architectures, and derivation of optimal design and energy management practices across a wide range of the operational envelope, and infrastructure capabilities. The project relates very strongly and directly to research areas under the Fossilfritt flyg 2045 programme.

Implementation

The major work packages of the project are listed below:

Work package 1 – Technology screening and requirements capture: Review and initial analysis of H2-powered and electrified aircraft architectures and modelling methods, energy conversion and distribution infrastructure requirements and regional market opportunities, and regional aircraft requirements and Swedish/Scandinavian market analysis.

Work package 2 - Aircraft and engine model development and system level integration: Development of mathematical models for individual components of the systems under investigation. Model benchmarking and validation. Integration of component models into complete engine/aircraft architectures. Development of reference and novel configurations. Definition of operational procedures and consideration of regional infrastructure capabilities and operational requirements.

Work package 3 – Ground infrastructure modelling and system level integration: Development of mathematical models for gasifier, membrane, electrolyzer, and fuel cell systems. Model benchmarking and validation through experiments on a pilot plant. Integration and performance analysis based on the requirements from aircraft configurations and the identification of infrastructure limitations and market opportunities.

Work package 4 – System-level assessments and technology down-selection: Definition of assessment metrics and key performance indicators (KPIs). Definition of design space bounds, optimization algorithms and exploration strategy. Design space exploration and identification of trade-offs. System-level energy optimization for the defined KPIs. Technology down-selection with consideration to the Swedish and Scandinavian context in terms of regional market and infrastructure.

Work package 5 – Project management, dissemination and communication: Project coordination, a final project report (internal and to financers) and external communication of results through dissemination activities, conference publications and journal articles.

All work packages were led by MDU with support from Saab AB and Modelon AB.

Results

Thermal powerplant and aircraft modelling

For the following investigation of the hybrid-electric and H2-fired configurations, modelling of the thermal powerplant, aircraft and mission follows the same methodology, independently of configuration. The baseline aircraft remains the same and is a small commuter of 19 passengers. Therefore, this approach is reported in this section and the distinct changes that are applied to generate the hybrid-electric and H2-fired architectures are mentioned.

For the conventional aircraft and the H2-fired one, the entire gas turbine propulsion system comprises two underwing-mounted turboprop engines. A two and- a-half spool geared turboprop engine is selected, comprising an all-axial gas generator compressor (GGC), an axial cooled gas generator turbine (GGT), and an axial uncooled free power turbine (FPT), connected to the propeller through a two-stage reduction gearbox.

For the hybrid-electric case, the twin-turboprop aircraft is also equipped with a rear fuselage-mounted electrically driven ducted fan (EFAN) to assist in propulsion. The aft fan operates in the presence of boundary layer ingestion. The aft-mounted fan can be powered by battery, fuel in turboelectric mode, or by any feasible share between these energy sources. Power can be injected into or extracted from the turboprops for parallel, turboelectric, or on-flight battery charging operation. The EFAN system consists of a single-stage low pressure ratio ducted fan that is driven by an electrical motor. This combination of powerplants generates the serial/parallel partial hybrid architecture and is selected for its design freedom and environmental potential through electrification. The conventional and H2-fired configurations are presented on the left side of **Figure 1**, while the hybrid-electric configuration with the respective architecture is shown on the right side of the figure.

Performance of the gas turbine propulsion system is assessed within the environmental assessment engine conceptual design tool [Kyprianidis, 2017], using a multipoint synthesis approach. The matching scheme is initially based on the solely turboprop paradigm described by Sielemann et al. [Sielemann et al., 2022]. Modelling of this engine architecture includes a single-speed propeller methodology deploying the momentum theory approach.

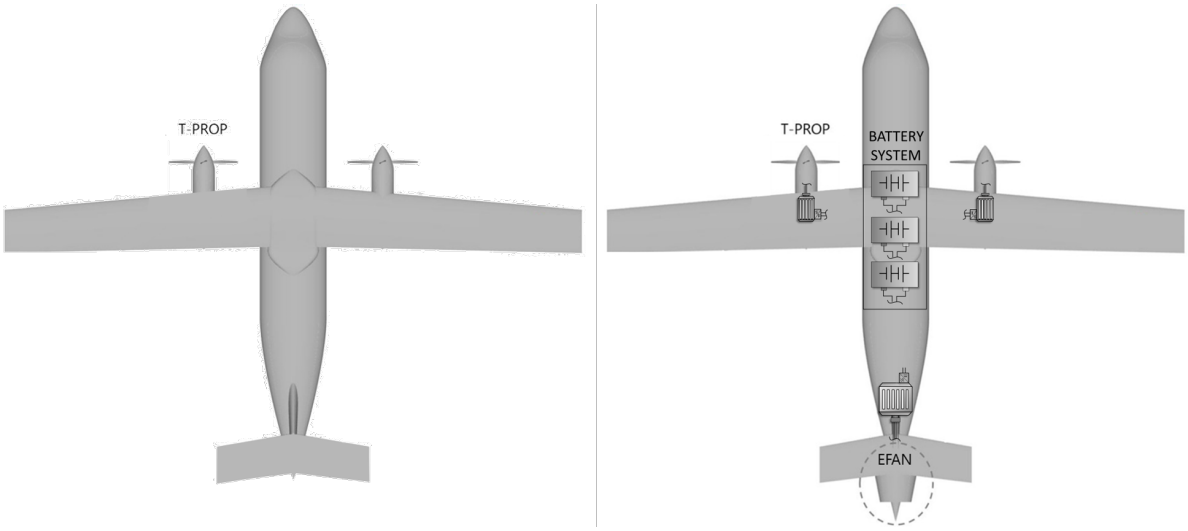

Figure 1. Jet-A and H2 aircraft configuration (left side). Hybrid-electric configuration (right side).

The performance matching scheme for the Jet-A and H2 turboprop engine includes six pairs of state and target variables and is shown in **Table 1**. The required GGT metal temperatures at end-of-runway Take-Off conditions are achieved through GGT rotor and stator cooling at Top of Climb. Cycle overall pressure ratio and combustor outlet temperature at cruise are kept at desired levels by iterating GGC pressure ratio and combustor outlet temperature at Top of Climb. Furthermore, the propeller rotational

speed at Top of Climb is iterated to achieve a propeller tip speed at Take-Off conditions, subject to established noise regulations. The converged propeller rotational speed is kept constant for remaining operating points. Regarding the reference point of Top of Climb, GG (Gas Generator) compressor inlet mass flow, and propeller tip diameter are iterated to satisfy propeller loading, as well as acceptable nozzle pressure ratio levels. An enhanced performance matching scheme is selected for the hybrid configuration. The EFAN is included in the matching scheme and EFAN power at Top of Climb is set as a target, matched with the EFAN inlet mass flow at the same point.

Table 1. Multipoint synthesis scheme for Jet-A and H2 burning engines. (NGV: nozzle guide vane, PR: pressure ratio, TOC: top of climb, T4: combustor outlet temperature, CR: cruise)

Targets	States
GGT NGV metal temperature	GGT NGV cooling flow
GGT rotor metal temperature	GGT rotor cooling flow
OPR @ CR	GGC PR @ TOC
T4 @ CR	T4 @ TOC
Propeller tip speed @ TO	Propeller rotational speed @ TOC
Propeller loading @ TOC	Propeller diameter
GG nozzle PR @ TOC	GG inlet mass flow @ TOC
EFAN Power @ TOC (only for hybrid-electric)	EFAN Inlet Mass flow @ TOC (only for hybrid-electric)

Sizing and weight estimation of the gas turbine propulsion system are also carried out within the environmental assessment conceptual design tool, which is based on the object-oriented Weight Analysis of Turbine Engines (WATE++) tool developed by NASA [Kavvalos et al., 2019]. Hot-day Top of Climb serves as design point of turbomachinery components.

Aircraft design and mission calculations are made withing the EVA tool [Tong et al., 2008] and are linked to the thermal powertrain model in a multidisciplinary framework. A predefined nominal aircraft dataset is used for dimension modelling of any new aircraft configuration [Jekinson et al., 1999]. Sizing and analysis of each airframe component is performed to reach an initial aircraft weight estimation [Roksam, 1985, Torenbeek et al., 2013]. Aircraft aerodynamics are modelled according to principes described by Jenkinson et al [Jekinson et al., 1999]. Aircraft drag polar is predicted during the mission for individual components based on aircraft geometry and high lift device settings. A rubberized aircraft wing model is used to capture the impact of different powertrain designs, weights, and installation locations on aircraft maximum take-off weight [HECARRUS project, 2022].

Aircraft performance modelling is based on methods described by Jenkinson et al. [Jekinson et al., 1999] and Roskam [Roksam, 1985]. The mission profile simulated comprises of take-off, climb, cruise, descent, approach, landing and taxi. Calculations include a main and diversion mission. All following results refer to main mission outcomes, however, inclusion of reserves and diversion mission in the design loop is fundamental as it impacts aircraft weight and aerodynamics. Cruise performance is calculated in a discretized manner to account for the on-flight fuel consumption, gradual reduction of carried weight, and therefore variation of thrust requirement. The aircraft dimensioning and weight calculations are coupled with the mission analysis and rubberized wing model to ensure the convergence of the needed fuel calculation, aircraft aerodynamics and final maximum take-off weight. By doing so, first order effects on the aircraft weight and wing design are incorporated into the final outcome. All design and business missions refer to 400 nmi, with 100 nmi of reserves.

A. Hybrid electric propulsion

Propulsion electrification is examined for mitigation of aviation's environmental impact. The serial/parallel partial hybrid architecture is selected for its design freedom and environmental performance potential.

A.1 Methodology

For the sizing of the electrical power system, an analytical methodology is developed. The detailed methodology is presented in great extend by Bermperis et al. [Bermperis et al., 2023]. The machine is designed to operate near saturation limit during peak requirements, which leads to a minimal material requirement for the stator and rotor sizing [Martinez, 2012, Laskaris, 2011, Woolmer et al., 2006, Rao et al., 2015]. Selection of cooling architecture closes the design loop, and a thermal resistance equivalent model is used to monitor temperatures during operation. For electric motor performance estimation, three loss generating phenomena are modelled [Magnussen, 2004]. These are copper, core, and windage losses. For the power electronic components, design is initialized at module level. A lumped thermal model is combined with sizing equations fitted to publicly available data for state-of-the-art components and scaled for the projected EIS year [Vratny et al., 2019]. Packaging and cooling surface masses are accounted for in the final sizing outcome. Performance of power electronic components is estimated in a time-average manner capturing conduction and switching losses [Infineon]. DC power cables and their insulation are sized according to ground application, and scaled to flight conditions, by catering for the impact of air density and ambient temperature [NFPA, 2014]. The sizing and performance model of the battery refers to Li-ion cells. Cell characteristics are scaled to pack-level accounting for auxiliary components and electronic connections. Heat exchange surfaces are designed to ensure battery operation under advised limits. A resistance-capacitance equivalent model is combined with a scaled Sheperd model for the battery system performance [Chen et al., 2006], allowing for representation of both charging and discharging conditions.

The integrated electrical power system of the examined hybrid architecture comprises of three distinct parts. A battery system and DC bus bar span the fuselage and act as an anchor point where all electrical power branches connect. The EM-EFAN sub-system refers to the electrical branch that is coupled to the aft-fan (EFAN) and drives it. An axial-flux permanent magnet synchronous motor is selected for its torque density and is coupled with a SiC DC/AC inverter for control. The GEN-GT sub-system refers to the electrical branch that is coupled to the gas turbine. A radial-flux permanent magnet synchronous machine is mechanically connected to the FPT and is used for power extraction, therefore acting as a generator. A SiC AC/DC rectifier controls the generator. A DC/DC converter connects the branch and DC bus bar. For both branches, power is transmitted through aluminum DC power cables.

Models for sizing and performance estimation of electrical power system components are integrated in a common framework. Details about the selected hybrid architecture are incorporated within the framework logic. Given a mission profile and hybridization strategy, a power and shaft speed profile is derived for the electrical drives that are connected to turbomachinery components. Power demand is passed through components of respective branches accounting for performance of individual components. Operating current and voltage are also estimated for each component. The EM-EFAN and GEN-GT branches are sized, and their performance is estimated. An iterative algorithm is created to ensure that battery system outputs converge to the calculated demand of the electrical branches. Actual battery system design relies on the duration of all mission segments. The framework delivers a fully sized electrical power system, with its performance predicted at all representative mission phases and with individual component maps available.

Representative power levels of specific flight envelope segments are shown in **Figure A1**. The resulting nominal hybridization scheme corresponds to the mid-point reference of **Table A2**, low-power design of **Table A3**, and slightly differs from mid-point reference of **Table A1** (climb EFAN power of 450kW instead of 475 kW). With a nominal design voltage of 500V, the baseline EPS weighs 1440 kg. The

GEN-GT branches contribute 105 kg, the EM-EFAN branch 190 kg and the battery system the remaining 1145 kg. In comparison, the gas turbines and aft fan weigh a total of 650 kg.

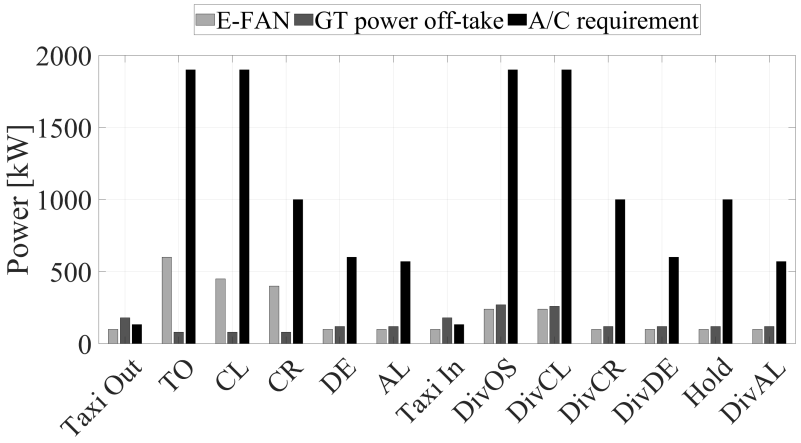

Figure A1. Representative power levels of mission segments.

Aircraft power requirement refers to the summation of propeller shaft and aft EFAN power output. The latter considers transfer losses from EFAN input power. EFAN power levels indicated in **Figure A1** refer to EFAN input power, irrespectively of energy source. Propeller shaft power relates to GT shaft power, accounting for mechanical losses. Power extracted from the gas turbine to drive the electrical power system and EFAN is noted as GT power off-take and is presented in absolute terms. Battery power is defined as the difference of EFAN power and GT power off-take, considering electrical transmission losses.

Cruise is the longest mission phase and holds great potential for environmental impact reduction through electrification. Similarly, Take-Off and climb are highly loaded segments, and hybridization offers potential consumption benefits. To isolate these effects, EFAN is operated in full turboelectric mode for other main mission phases. Diversion is to be conducted with one energy source.

A.2 Results

Influence of turbomachinery design point

A parametric analysis is performed for three climb EFAN power levels. For each case, EFAN power at climb remains constant. Given the powertrain architecture and mission constraints, the reference point is set at 475 kW and corresponds to the EFAN operability range mean. A +/-25% change defines the upper and lower values of the study. Selected climb EFAN power levels correspond to 14.2%, 20.8%, and 27.4% degree of power hybridization. **Table A1** shows the impact on sizing of electrical components and complete branches.

Motor design point power requirement is constant. However, power at Top of Climb for turbomachinery components and climb for EPS are connected. As EFAN power at climb increases, its size does also. Yet, power input at Take-Off remains constant. This forces the EFAN to operate at a lower rotational speed during that phase. Take-Off is the designated electric motor design point. The design rotational speed reduction allows the electric motor to be designed with a larger diameter since its structural tip speed limit is constant. An axial-flux machine is benefited from a larger diameter, and its specific power increases. Design point efficiency also changes, and design power of other components connected to the machine is affected. The initial change in EFAN rotational speed at Take-Off has a propagating effect on EM-EFAN branch design. A +/-25% change in EFAN power during climb does not have a symmetric effect on electrical branch sizing, indicating non-linearity in electrical component design. A 5.9% penalty and 4.1% benefit in branch mass are reported, with respect to the selected levels of EFAN

power at climb. The EFAN change has different impact on components, thus mass and specific power deltas differ slightly.

This case study's design variable directly correlates to EFAN design. Nevertheless, the integrated powertrain leads to an influence on the GEN-GT branch as well. Given a constant A/C power requirement, changing power split between EFAN and propellers affects sizing of both. As EFAN power at Top of Climb increases, propeller power requirement at that point drops. In the GEN-GT branch, a 1.4% benefit and penalty in branch mass are reported from a respective increase and decrease of design speed. The extended study for this electrical branch is presented by Bermperis et al. [Bermperis et al., 2023]. A 25% increase of climb EFAN power is beneficial for electrical branches with a mass decrease in the order of 3.5%. However, fuel-powered propulsion system dry mass increases in the same order. These masses are comparable, hence the impact on overall power system weight is equalized.

Table A1. Sizing parameters of electrical branches for different EFAN power levels at climb.

Variables & Metrics	Units	Studied Cases		
EFAN Power @ CL	[kW]	350	475	600
DoH Power @ CL	[%]	14.2	20.8	27.4
Power Split @ CL	[%]	18.4	25	31.6
EM - EFAN branch				
Design Power	[kW]	600	600	600
Design Speed	[rpm]	3715	3375	3155
Design Torque (per stack)	[N.m]	514	849	908
Stacks	[-]	3	2	2
Delta[Mass branch]	[%]	+5.9	0 (184 kg)	-4.1
Delta[SP branch]	[%]	-5.6	0 (3.3 kW/kg)	+4.2
GEN - GT branch				
Design Power	[kW]	162	162	162
Design Speed	[rpm]	21387	22146	22977
Design Torque	[N.m]	72.3	70	67.3
Delta[Mass branch]	[%]	+1.37	0 (45 kg)	-1.41
Delta[SP branch]	[%]	-1.35	0 (3.6 kW/kg)	+1.43

For the design variables of **Table A1**, impact on performance during significant operational segments is examined. EFAN power during cruise is varied and EM-EFAN efficiency is monitored. The variation of EM-EFAN branch efficiency and machine rotational speed for a range of EFAN power at cruise and climb is shown in **Figure A2 (left)**. Variation of cruise power corresponds to 10-50% EFAN power contribution. Degree of hybridization is subject to actual mission operation. Three operational speed curves are indicated with grey lines. A step change between them arises from the impact of climb EFAN power on electric motor design speed. As cruise EFAN power increases, rotational speed does also to cope with the rising demand. As branch operating power remains around 50-100 kW, power losses are also low in absolute terms despite the efficiency drop. As both power and speed load increase, the machine and electrical branch operational point shifts towards the optimum efficiency island. A point of optimal performance lies in the range of 40-60% loading. Above this threshold, performance penalties, with a respective efficiency drop of 2-3 percentage units, are inflicted. The main driving factor of EM-EFAN branch performance is the electric motor. Inverter operates at 98-99% efficiency and follows the trend of branch performance. DC power cables have efficiency in the order of 99.8%.

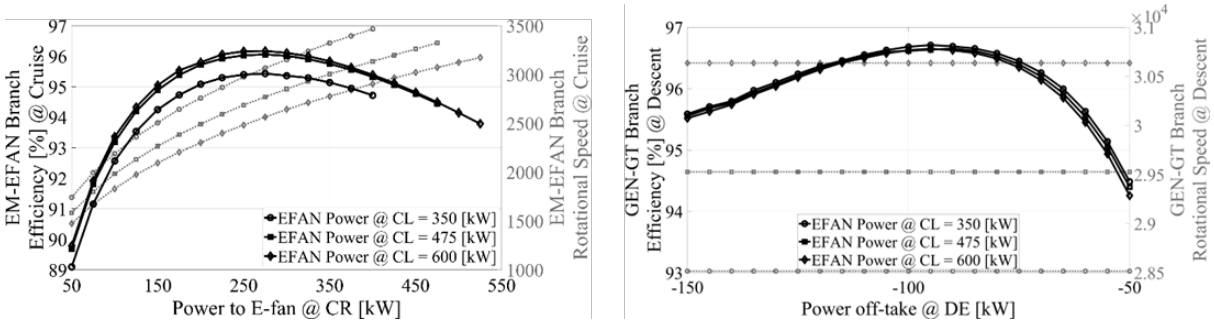

Figure A2. EM-EFAN branch operation and performance for varying EFAN power contribution at cruise and climb (left). GEN-GT branch operation and performance for varying GT power off-take at descent and climb EFAN power (right).

The GEN-GT branch is considered to unlock the potential of on-flight battery charging. Despite branch utilization during segments of turboelectric operation, in this work descent is examined as the operationally significant phase. The opportunity of charging at descent arises from the low aircraft and EFAN power requirement, which enables the branch to power the EFAN and charge the battery, simultaneously. The variation in GEN-GT performance during descent is highlighted in **Figure A2 (right)**. FPT power off-take to generate electrical power for the branch is varied from -150 kW to -50 kW. Negative sign results from the used sign convention. Higher absolute value corresponds to greater power extraction. Three distinct and flat operational speed lines are shown with grey for respective EFAN power levels at climb. The relatively small deviation between operational speed levels has an equally small effect on generator performance. From the perspective of electrical losses, a properly sized and operated GEN-GT branch holds potential when considered for on-flight battery charging.

A +25% change in climb EFAN power has a small impact on EPS branch performance, of about 0.5 percentage units. Turbomachinery component efficiency and consumption rates are impacted more. Propulsive and overall efficiency of the conventional propulsion system increase by 2 and 1 percentage units, respectively, while installed SFC drops by 2.5 percentage units. As long as electrical branch mass benefits compensate for increased conventional propulsion system mass, and operability margins allow, increasing climb EFAN power yields worthwhile performance benefits for the integrated power system.

Influence of EPS design point

Each electrical branch is designed for a specific power level which is determined by the most demanding conditions during mission. In this section, the design segment is fixed so that no unexpected interactions take place. EM-EFAN branch design is set on Take-Off, which has the greatest A/C power requirement and consequently peak electrical boosting can be utilized. GEN-GT branch design depends on the operational requirement of one energy source at diversion mission. Diversion overshoot is the GEN-GT design point. Impact of design on performance is examined with branch efficiency at segments of operational significance for a range of power levels.

Sizing design variable and EM-EFAN branch outcomes are presented in **Table A2**. Three distinct levels of different EFAN power at Take-Off are examined. The 600 kW mid-point of the feasible range is selected as reference. A +/-25% change is applied to define the upper and lower study bounds, respectively. The selected power levels correspond to 19.5%, 27.4%, and 35.3% degree of power hybridization.

EFAN power input and electric motor design power match. EFAN power at Top of Climb is fixed for this study. EFAN size does not change for varying power input at Take-Off and the increase in EFAN power requirement is matched by an increase in EFAN rotational speed. Direct coupling of electric motor and EFAN imposes a respective increase of electric motor design speed. Multiple effects take place during EM-EFAN branch sizing when design point power levels vary. Electric motor sizing

depends on both power and speed. Moreover, design power of all branch components changes with respect to EFAN power. Power losses of each component accumulate to the design power of previous components to deliver the EFAN power requirement. Overall, design power is the driving factor of electrical branch mass.

Table A2. EM-EFAN sizing for different design power levels.

Variables & Metrics	Units	Studied Cases		
EFAN Power @ TO	[kW]	450	600	750
DoH Power @ TO	[%]	19.5	27.4	35.3
Power Split @ TO	[%]	23.7	31.6	39.5
Design Power	[kW]	450	600	750
Design Speed	[rpm]	3166	3447	3695
Design Torque (per stack)	[N.m]	679	831	646
Stacks	[-]	2	2	3
Delta[Mass branch]	[%]	-32.7	0 (189 kg)	+22.8
Delta[SP branch]	[%]	+11.5	0 (3.2 kW/kg)	+1.8

A 25% reduction in design power is accompanied by an 8% reduction in design rotational speed. An axial-flux motor can be benefited by reducing design speed, since a larger diameter may be used. Hence, a more power dense machine is available. With constant system voltage, a drop in design power corresponds to a decrease in design current for the inverter. Usually, reduced current means fewer losses and a more compact design. However, power drops as well, negating the benefits of reduced current in terms of specific power. On the other hand, as design power drops, active PEC sub-components are downsized. Packaging and inactive material contribute more to overall mass, negatively impacting specific power. Finally, a decrease in design power corresponds to reduced design current for the DC power cables. This decrease has a small effect on specific power of the conductor due to the proportional drop in design current and power. However, conductor radius decreases, which with constant voltage results in less insulation and protection sleeve mass. This benefits specific power of DC power cables. Overall, a drop in design power level leads to a more power dense system. Thus, mass reduction is not solely dictated by design power but also the impact on specific power. A 25% increase in design power leads to a 7% rise in design rotational speed. One more motor stack is added to cope with increased requirements. Compared to the 600kW motor, mass and power output increase proportionally resulting in little effect on electric motor specific power. Overall, specific power increases, but less than the -25% design power branch. Branch mass is affected by the increase in design power, and slightly benefited from the increase of specific power.

Sizing parameters and outcomes from the GEN-GT branch design point parametric analysis are presented in **Table A3**. Diversion overshoot is the designated branch design phase due to the one energy source requirement in diversion and EFAN operability range. 135 kW power off-take sets the lower bound. A mid-point reference power level and upper bound are defined to be consistent with the 25% variation in all design variables presented thus far. Power off-take refers to power extraction from the turboprop FPT via the directly coupled generator.

The connection of gas turbine and GEN-GT branch happens at the generator, where branch design is initialized. Therefore, all design aspects of the generator are presented as their impact in following components is of interest. For redundancy and safety reasons, a 20% oversizing on torque and power is imposed on the generator and branch design. Consequently, generator design power is higher than the overshoot segment power off-take.

Power and torque critical conditions for branch design may arise from different mission segments. While overshoot has been assigned as the most power demanding phase for this branch, peak torque requirement comes at taxi for the -135 kW and -180 kW designs. A considerable power off-take during taxi along with low FPT speed result in high torque input. The electric machine shall safely operate in both critical conditions, thus their combination generates design speed. On the highest examined level of design power, critical torque and power conditions arise at diversion overshoot, hence design speed matches the respective FPT speed.

A 25% increase in branch design power results to more power dense components by 6.2%. Opposite trends and sizing principles are active on the -25% design power case, where branch specific power drops by 14.1%. The asymmetry in relative deltas corresponds to the constant design torque which generates a greater design speed reduction. Specific power is penalized, and mass reduction benefits are less for the same relative change in design power. Overall, branch mass is driven by design point power. However, different power levels imply different branch specific power, which affects the final mass outcome. Therefore, the +/-25% change in design power results in a 17.7% and -12.6% change in branch mass, respectively.

Table A3. GEN-GT branch sizing for different design power levels.

Variables & Metrics---	**Units**	**Studied Cases**		
Power off-take @ DivOS	[kW]	-225	-180	-135
Design Power	[kW]	270	216	162
Design Speed	[rpm]	32204	29276	21957
Design Torque	[N.m]	80	70.5	70.5
Delta[Mass branch]	[%]	+17.7	0 (51.5 kg)	-12.6
Delta[SP branch]	[%]	+6.2	0 (4.2 kW/kg)	-14.1

Cruise is the longest segment and holds great potential for benefits in consumption and emissions through electrification. Thus, EM-EFAN performance is monitored for different levels of EFAN power at cruise and Take-Off. Three curves in black are illustrated in **Figure A3 (left)** for the performance of each design power level. Three identical grey curves indicate the variation in electric motor speed for the cruise EFAN power range. Electric motor operational speed is dictated by the EFAN rotational speed requirement. Take-Off EFAN power has no effect on EFAN speed at cruise. An increase of cruise EFAN power results in an increase of rotational speed, so that more mass flow passes through. Performance of the EM-EFAN branch is affected by a simultaneous change in speed and power loading. Below the point of gradient switch in the performance curve, efficiency improves with loading. The range that this effect takes place for each designed branch is different. On the given cruise EFAN power range, a high-power design experiences lower loads. Once optimum performance is passed, loading increases slightly more, yielding small performance losses. On the other hand, a low-power design is loaded relatively more and quickly reaches optimum performance in the examined feasible range. Although, this design has better efficiency in this range due to higher relative loading, above the optimum point, increasing cruise EFAN power rapidly penalizes performance.

A trade-off in performance and sizing is recognized. Given the maximum feasible power setting of the EFAN, it may be prudent to oversize the electrical branch, if high degrees of hybridization are of interest. This forces the operational point of significance into a better performing range for electrical components. At the expense of increased branch weight, fewer power losses are propagated to the battery. Given their unfavourable power and energy density, oversizing the electrical drives could be beneficial at aircraft-level. Take-off requirements shape the range of feasible power loading of turbomachinery components in other segments. Given the small impact on conventional propulsion system dry mass and performance, Take-Off EFAN power could be selected according to EPS needs for optimal mission-level outcomes. Descent has been established as the phase of operational interest

for the GEN-GT branch due to the potential of on-flight charging. Three performance curves in black for different overshoot segment power off-take levels, and branch designs are illustrated on **Figure A3 (right)**. For the same range of operational power, different design power leads to different relative power loading. Thus, a high-power branch has lower relative loading. Detailed analysis of interrelationships is presented by Bermperis et al [Bermperis et al., 2023].

The same trade-off between electrical branch mass and performance is recognized, as with the EM-EFAN branch. It may be beneficial to oversize the GEN-GT branch to achieve better performance at a highly loaded segment which is of interest. In this study, descent has been the segment to optimize around. However, there is a significant part of mission when the GEN-GT branch operates at very low loads.

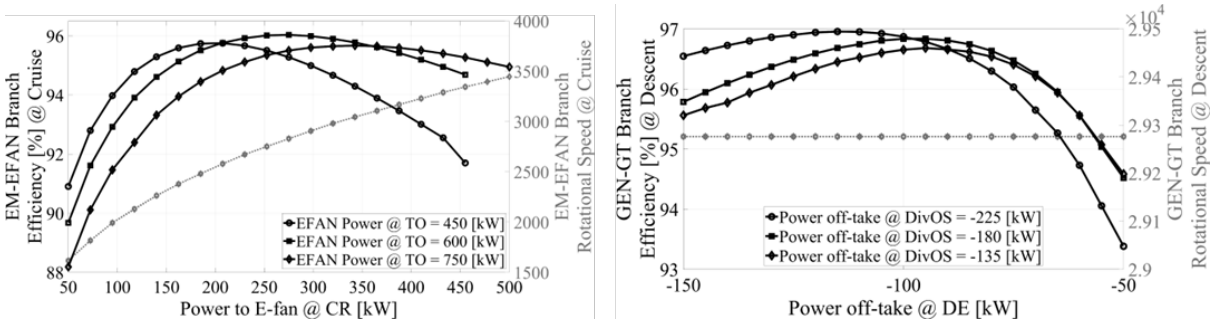

Figure A3. EM-EFAN branch performance and operation for varying EFAN power contribution at cruise and Take-Off (left). GEN-GT branch performance and operation for varying GT power off-take at descent and diversion overshoot (right).

Influence of system voltage

System voltage plays significant role in performance and design of electrical components. Potential benefits can be realized by studying system and component dependencies. The change in branch mass for varying system voltage is presented in **Figure A4**. The upper and lower bound of electrical branch design power are part of the parametric analysis to examine interactions between branch design voltage and power. The EM-EFAN branch indicates mass reduction up to 50% for a maximum 2kV value, while the GEN-GT up to 10%. While all components are affected by increased voltage, DC power cables drive this outcome. The EM-EFAN DC power cables contribute an order of magnitude more to branch mass than the respective GEN-GT component due to greater design power and length. Therefore, EM-EFAN branch mass reduction is greater.

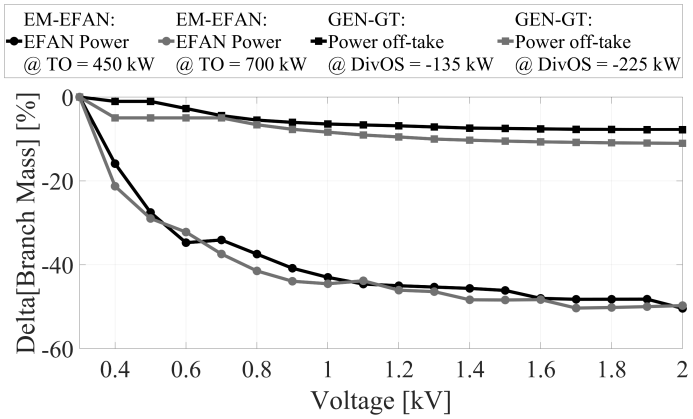

Figure A4. Change in branch mass for varying system voltage and EPS design point requirements.

Little mass reduction benefits are realized above the 1-1.2kV range. A voltage increase for constant branch design power leads to a proportional drop in current. Current is a significant driving factor in

electrical component design, but not the only one. As it reduces to low values for high system voltage, current related mass benefits saturate. The complexity of designing high voltage systems keeps ramping with voltage. Arcing issues in components, need for thicker and heavier insulation, component proximity considerations, and limitations in aviation suitable and available components are some predominant obstacles. Therefore, going above the threshold of 1kV may be an unreasonable and unrealistic design choice for an EIS 2035 configuration.

Aircraft and mission performance

Three reference configurations are designed in this study in order to connect currently available and flying aircraft with the projected advances in technology and future aviation goals. Given that many of the current environmental objectives of the aviation industry have been set during the previous two decades, an aircraft with EIS 2014 is set as the primary reference case. This is a virtual airplane, matching state-of-the-art technology of that period. The EIS 2035 conventional aircraft is designed to verify and isolate the impact of technological improvements for conventional aircraft during this 20-year period. Finally, the hybrid EIS 2035 design brings perspective to the impact of electrification compared to an advanced conventional design. It also acts as the starting point for any following investigations regarding hybrid aircraft in this work.

Table A4. Performance metrics for reference configurations.

	Units	Conventional		Hybrid
		EIS 2014	EIS 2035	EIS 2035
Top Level Requirements				
MTOW	(%)	Ref.	-17.0	+8.0
TOFL [SL, ISA]	(%)	Ref.	+11.2	+9.1
Climb Rate [SL,ISA,AEO]	(%)	Ref.	+13.7	-1.8
Mission Performance				
Block Fuel	(%)	Ref.	-28.6	-17.9
Block El. Energy	(kWh)	-		400
Block Energy	(%)	Ref.	-28.6	-18.2
Block CO2	(%)	Ref.	-28.2	-17.8
Block NOx	(%)	Ref.	-34.4	-25.1
Thermal Powerplant				
PWSFC @ CR	(%)	Ref.	-20.1	-27.9
PWSFC @ TOC	(%)	Ref.	-16.0	-32.3
Propeller Loading @ CR	(%)	Ref.	-29.2	-58.8
Dry Mass GT	(%)	Ref.	-36.1	-33.3
Dry Mass Propeller	(%)	Ref.	-21.9	-9.4
Electrical Powerplant				
Battery Mass	(kg)	-		920
Battery Energy Cap.	(kWh)	-		520
Total EPS Mass	(kg)	-		1180
Motor Drive Sp. Power	(kW/kg)	-		5.6
Aircraft				
Wing Loading	(%)	Ref.	+27.5	+15

Key performance metrics for these three reference configurations are presented in **Table A4**. Improvement in materials technology leads to a lighter conventional EIS 2035 aircraft compared to its EIS 2014 counterpart. Despite that, the hybrid aircraft carries significant battery mass resulting in increased MTOW, but still within certification limits. Wing design is chosen such that take-off and climb performance satisfy top-level requirements.

Specific fuel consumption benefits in the order of 20% and 28% are realized for the conventional and hybrid EIS 2035 aircraft, respectively. This reduction is driven by the increase in turbomachinery efficiency and the hotter and higher OPR cycle that these are designed for. The hybrid aircraft gains an additional 8% improvement of fuel consumption compared to its conventional counterpart due to the addition of the battery-powered driven aft fan, while the gas turbine design power conditions stay constant. In terms of mission outcomes, gas turbine performance and the respective change in MTOW along with the constant mission design range lead to block consumption and emissions reduction for the EIS 2035 designs compared to the conventional EIS 2014 aircraft. However, the reference hybrid aircraft underperforms compared to its conventional counterpart which is a direct effect of battery weight on overall aircraft mass. Despite the specific fuel consumption benefits for the hybrid, the added battery mass dominates the outcome of block consumption. Block emissions closely follow these trends as they are much dependent on conventional fuel consumption.

For the hybrid configuration, battery mass contributes to 78% of the overall electrical power system, which in turn is about 14% of maximum take-off weight. Hence, to achieve around 20% degree of power hybridization, the resulting battery mass weighs twice as much as the consumed block fuel. Accounting for the packaging and auxiliary components of the battery system, the specific energy comes to 0.56 kWh/kg which is a 13% reduction compared to the projected specific energy of the cell for the EIS 2035 assumed technology. Finally, the resulting design of the electrical drive that is coupled to the EFAN has a specific power of 5.6 kW/kg.

By assessing the relative change in performance metrics between the conventional and hybrid EIS 2035 designs, it becomes apparent that optimal power management strategies and proper employment of the electrical power system is necessary for the latter to become competitive. Careful exploration of the design space and effective utilization of the integrated power system is crucial in exploiting the full potential of any complex hybrid architecture.

Power management strategies for EIS 2035 designs

A design space is defined through power settings of the electrical aft fan and gas turbines, which are the main variables of interest in the pursuit of guidelines for optimal power management strategies. Around 5000 points have been selected with the Latin Hypercube Sampling method and simulated. Examined ranges and corresponding degrees of hybridization during those mission segments are presented in **Table A5**. Degree of hybrization is defined as the ratio between electrical power delivered to EFAN from the battery over the total aircraft power requirement. Selected range limits are indicative of design feasibility for the thermal and electrical components.

Table A5. Power setting and degrees of hybridization for the design space .

	Lower bound	**Reference**	**Upper bound**
	EFAN Power (source: battery) [kW]		
Take-off	220	420	660
Climb	200	400	600
Cruise	50	200	350
	Aircraft Power Requirement [kW]		
Take-off		2200	
Climb		2000	
Cruise		1000	
	Degree of Hybridization for Power [%]		
Take-off	10	19	30
Climb	10	20	30
Cruise	5	20	35

An optimal power management strategy is one that results in minimum block fuel and energy consumption. It should also yield minimal emissions during flight. This study considers CO2 and NOx emissions. For a design to be acceptable, top-level and customer requirements need to be met. Given the complexity of the design space and number of constraints imposed on the problem a set of relaxed constraints is also defined and the subsequent filter is employed in the investigation. The initially selected and relaxed limits are presented in **Table A6**. The purpose of this is to evaluate the trends of performance metrics at their completeness and assess whether despite the adverse effect of battery addition, there is further untapped space to capitalize on electrification benefits.

Table A6. Design space exploration set and relaxed constraints of top-level requirements.

	Constraint	**Relaxed Constraint**
SOC [%]	≥ 20	≥ 15
MTOW [kg]	≤ 8618	≤ 9050
RoC [ft/min]	≥ 2150	≥ 2000
TOFL [m]	≤ 800	≤ 1000

A multitude of points from the design space are simulated, each representing a different aircraft design. From around 5000 different designs, the best performing ones in terms of block fuel and energy consumptions are collected and presented in comparison with the reference hybrid design in **Figure A5**. For this case, best performing designs are deemed those that achieve the greatest savings for given power settings, while depleting the designed battery fully, irrespectively of size. The best performing designs constrained with the initial limits reveal that acceptable ones reach EFAN power of 460 kW, 440 kW, and 365 kW, which correspond to degrees of hybridization of 19%, 20%, and 20% for take-off, climb, and cruise, respectively. Despite the use of twice as light batteries in designs of low degree of hybridization (5-10%), neither block energy nor block fuel reduction is possible. Less battery capacity directly translates to less electrification and greater share of chemical energy in the overall mix.

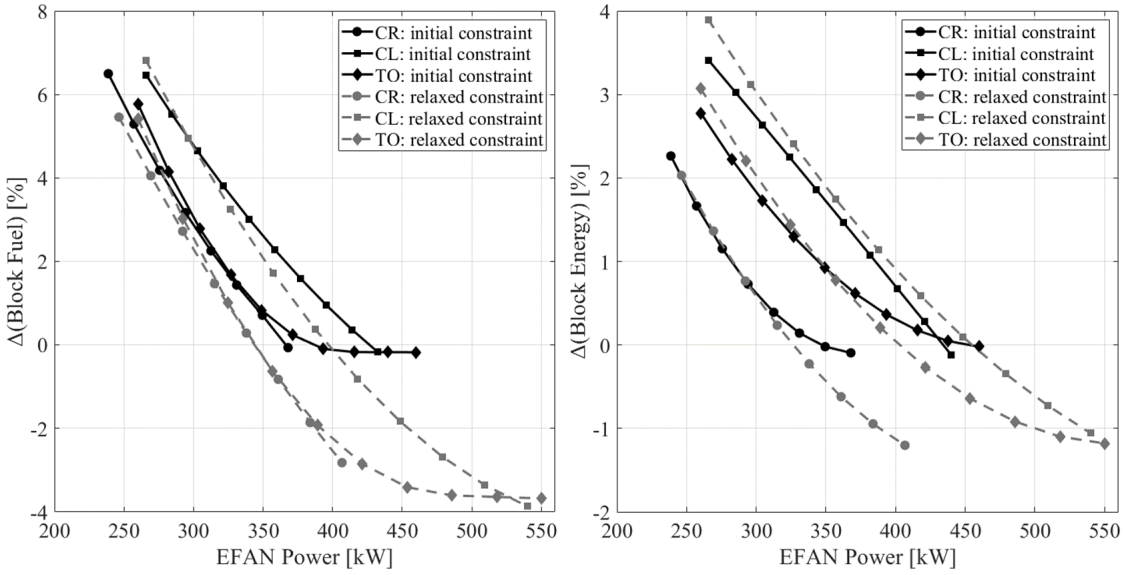

Figure A5. Block fuel (*left*) and block energy (*right*) consumption of best performing designs for initial and relaxed constraints with respect to EFAN power.

Yet, even the best emerging power management strategies do not yield further fuel and energy saving compared to the reference hybrid design. Relaxing the constraints allows for acceptable design of up to 550 kW, 550 kW, and 425 kW of EFAN power, which correspond to degrees of hybridization of 23%,

25.5%, and 27.5% for take-off, climb, and cruise, respectively. Those designs yield a further 3-4% reduction of block fuel and 1% reduction of block energy compared to the reference hybrid case. This trend implies the potential suitability of the examined hybrid architecture for bigger aircraft, such as in the regional class. Battery mass bounds of 1000 kg and 1300 kg for the regular and relaxed limits, respectively, are calculated. Both power density and energy density of the battery are of importance and critical for the design.

To further highlight the importance of a fully depleted battery and connect metrics of interest, **Figure A6** relates the differences in maximum take-off weight and block fuel consumption. All simulated points are presented, and a color filter indicates whether they are acceptable designs and under which constraints. Maximum take-off weight and block fuel consumption constitute competing objectives and a Pareto front from the best performing designs is constructed and presented in **Figure A6**. Moreover, it is verified once again that with the given technology assumptions and top-level aircraft requirements, it is very difficult to achieve further consumption benefits from what the reference hybrid design provides.

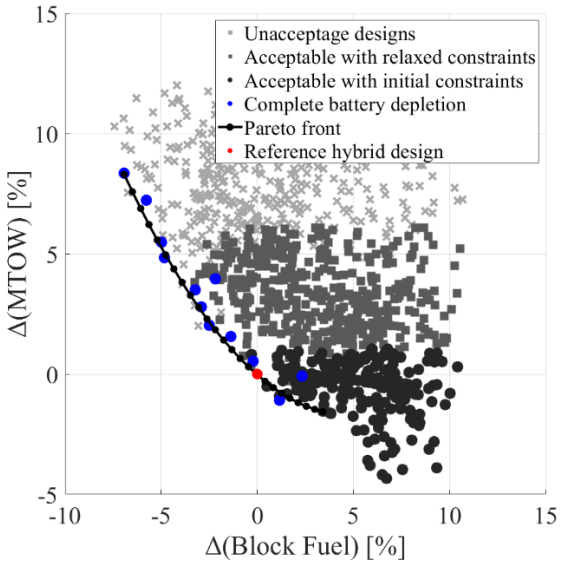

Figure A6. Pareto front between MTOW and block fuel consumption for the investigated objective space.

The overall performance of the gas turbines and electrically driven aft fan are presented in **Figure A7**. For the thermal power systems, EFAN power at cruise and climb show greatest impact on overall efficiency due to their role on the multipoint synthesis scheme. As EFAN power at climb increases, design power at top of climb increases for the EFAN and decreases for the gas turbines, due to the constant aircraft power requirement at that point. Increasing EFAN power at cruise corresponds to decreasing gas turbine power at the same phase.

In terms of gas turbine overall efficiency, improvements emerge in the area of increased climb EFAN power and decreased cruise EFAN power. This combination represents a lower power design gas turbine with higher relative loading during cruise. As EFAN power at top of climb increases, the aft fan is designed larger with a positive effect on propulsive efficiency. A decrease in cruise EFAN power translates to lower fan pressure ratio for constant EFAN design, which again leads to better propulsive and overall EFAN efficiency.

Therefore, to maximize thermal powerplant efficiency, the designer of these systems would aim to achieve a high degree of hybridization on the design point and combine it with low degree of hybridization during cruise. This indicates a large EFAN and smaller gas turbines and propellers, with relatively higher cruise loading for the gas turbines and lower for the EFAN.

For the electrical branch, cruise performance depends on the relation between branch design power and loading. The electric motor impacts branch performance the most. Optimal performance is achieved in

the region of medium to low cruise loading with respect to the design point that usually comes from the take-off power setting, given that EFAN and aircraft power are greater there. However, this region of the design space mainly involves configurations where batteries are not fully depleted. Therefore, the objective of the electrical power system designer becomes to select such a loading during cruise that will fully deplete the designed battery in the most efficient manner. This is achieved by having a ratio of at least 1:1 between cruise and take-off degree of hybridization and an average minimum of 1:1.35 between cruise and take-off EFAN power for the examined design space, with potential of further increasing cruise hybridization. This is the marginal line of acceptable hybrid designs and the space of optimal load and design power settings for the electrical power system.

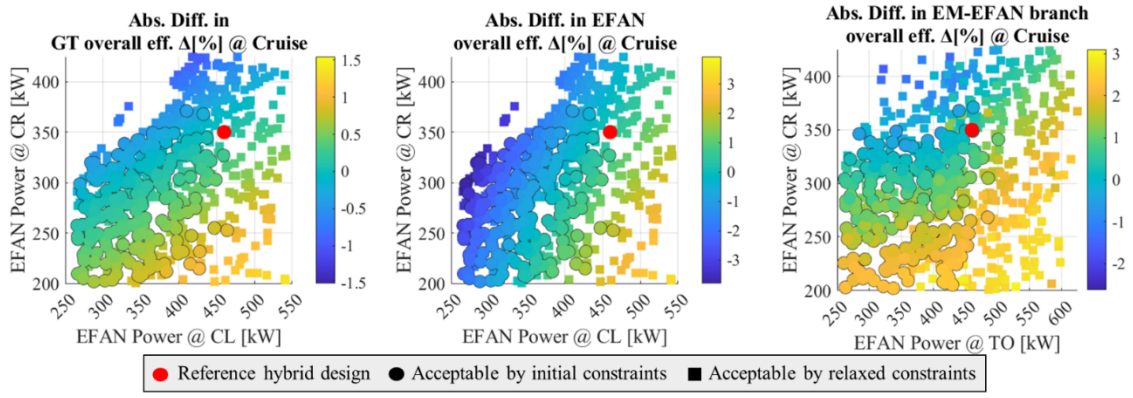

Figure A7. Thermal and electrical powerplant performance at cruise.

Analysis of the individual power systems indicates a common area of performance optimality which is defined by high take-off and climb EFAN power and low cruise EFAN power. In terms of battery depletion, however, this area corresponds to suboptimal electrical energy utilization and results in large battery designs where cruise electrification is not enough to take advantage of stored energy. As indicated by the curves of **Figure A5**, such a power management strategy is not optimal and does not yield any further consumption benefits. For optimal energy utilization and maximization of consumption benefits both the designer of the thermal and electrical power system should aim for as much electrification is possible in all mission segments. Achievable hybridization is limited by the selected customer requirements and top-level constraints, and the overall impact of increasing battery mass on aircraft performance. Despite this strategy not being optimal in terms of individual system performance, electrification results in enough fuel and energy savings to make it the overall best power management scheme for the examined space, aircraft architecture and mission profile. Hence, the designer of a commuter series/parallel partial hybrid electric aircraft should strive for as much hybridization as possible, while having a cruise to take-off or climb hybridization power ratio of at least 1:1.35, with the potential of increasing cruise power even further for given power settings in the other segments. This corresponds to a marginal ratio in degrees of hybridization between cruise and take-off or climb of 1:1.

The objective space and trends for emissions of CO2 and NOx are presented in **Figure A8**. Relative difference in block CO2 and NOx emissions compared to the reference hybrid design is shown. Both emission gases are closely related to block fuel consumption, therefore increased hybridization, especially during cruise which contributes the most to consumption, is a driving factor for the revealed trend. For designs of lower degree of hybridization compared to the reference case emissions of CO2 and NOx increase up to 10%. On the other hand, the relaxed design space allows for greater degrees of hybridization and reduced fuel consumption, therefore further emissions reduction up to 3% are achievable.

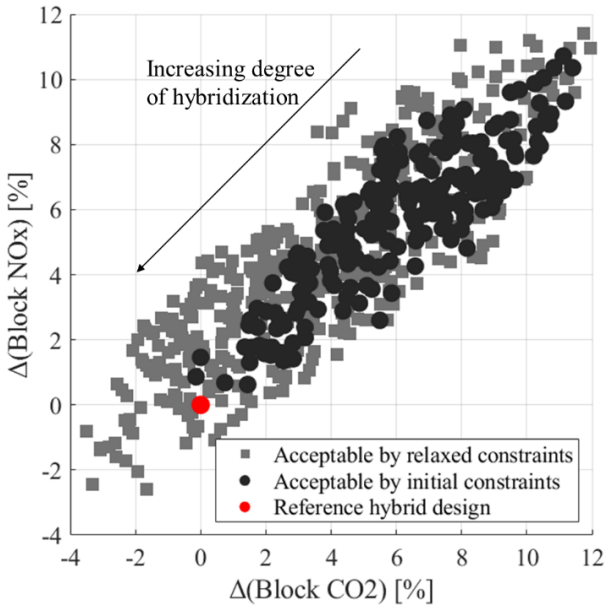

Figure A8. Relative difference of block CO2 and NOx emissions for simulated cases.

A sensitivity analysis with the purpose of generating exchange rates for the impact of the battery system and hybridization on the final hybrid-electric aircraft configuration and its environmental performance is conducted. The following exercise refers to the reference hybrid-electric aircraft of EIS 2035.

Therefore, the left column of graphs in **Figure 9**, presents a 1% increase in battery system mass and its impact. Given the cell specific energy assumption made herein, this mass increase results in a 0.85% increase of stored and available electrical energy, which emerges from the packaging and auxiliary battery system components mass penalty. It is noted that at this stage of the analysis it is assumed that the added energy is not consumed, and we strictly investigate the impact of battery mass on aircraft performance. Maximum take-off weight increases by 0.15% and with a fixed propulsion system. The associated added battery mass also impacts block consumption and emissions. Fuel, energy, and CO2 all increase by about 0.05% while NOx by about double that amount. Moreover, a 1% increase in battery mass reflects to a 0.78% increase of total EPS mass, showcasing the share of battery in overall electrical components, and perhaps the reduced impact that increasing specific power of electrical drives has on the final outcome.

On the right column graphs of **Figure A9**, utilization of the previously investigated added electrical energy is examined. It is assumed that the most plausible way to consume that energy is through extra electrification of the cruise phase. Therefore, a 0.72% increase of EFAN power at cruise is implemented, in order to expend exactly the added electrical energy. Direct effect of further hybridizing cruise is the reduction of consumption and emissions. Block fuel reduces by 0.125% leading to an aggregated benefit of 0.08% in terms of fuel consumption, accrued by the 1% increase in battery mass. Respective cumulative benefits are also present for CO2 and NOx emissions. The sensitivity analysis indicates that block energy consumption does not improve nor deteriorates for the examined infinitesimal space. This agrees with the plateau described by the block energy curves of **Figure 4**. Even though performance benefits are achieved, an increase of maximum take-off weight is unavoidable for hybrid-electric aircraft. The cumulative effect of this exercise results in an increase of MTOW by 0.13%.

Introducing some values for perspective, the conducted analysis showed that the addition of about 9 kg of battery system mass leads to the increase of stored electrical energy by 4.5 kWh but has come with an aircraft mass penalty of roughly 11 kg. Therefore, creating a potential metric to showcase the effect of adding electrical energy on the aircraft mass. This metric emerges at a value of 2.5 kg of aircraft mass per kWh of electrical energy added, not accounting for ‘snowball effects’ caused by large extrapolations of the exchange rates. Finally, adding and expending 4.5 kWh of electrical energy reduces block fuel consumption by 0.6 kg, which corresponds to avoid using 1.6 kWh of chemical energy for every kWh of electrical energy installed and used.

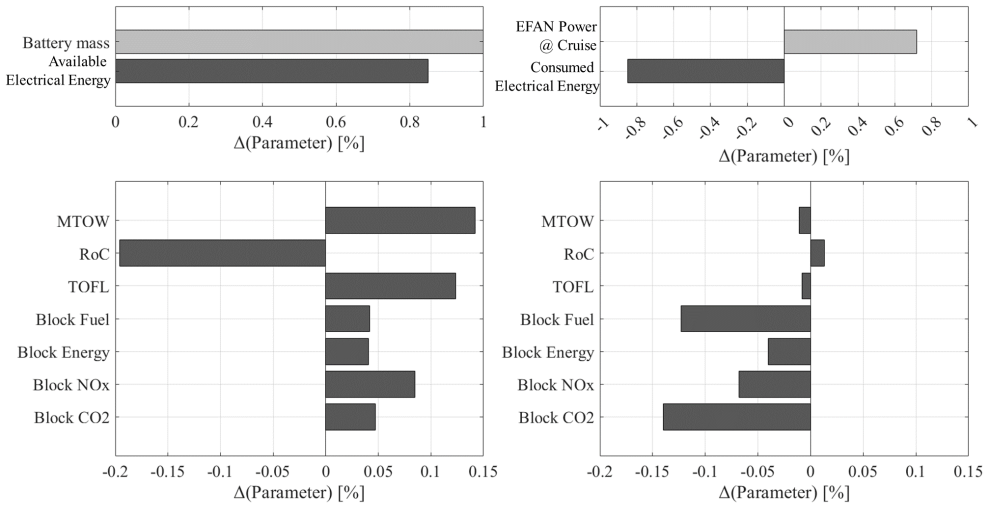

Figure A9. Sensitivity analysis of aircraft performance.

B. Hydrogen propulsion

Hydrogen propulsion is examined for its potential to reduce the environmental impact of aviation. A straightforward way to use H2 in the aircraft is by direct combustion of it in the gas turbine.

B.1 Methodology

For the direct burning of H2 in the gas turbine, Jet-A has been swapped with H2. The H2 fuel is assumed to be in gaseous form at the time of injection. The effect of the gaseous H2 temperature and pressure at the time of the injection is not explored in this study and fixed values are assumed for following calculations. The lower heating value of H2 is fixed at 120 MJ/kg with a constant specific heat capacity of 14.55 kJ/(kg.K).

It is assumed that H2 is stored in the aircraft in liquid form. Srinath et al [Srinath et al., 2022] presented a high-level investigation of hydrogen tanks and the associated thermal management systems that are necessary for fuel conditioning. Winnefeld et al. [Winnefeld et al., 2018] presented a detailed analysis for the estimation of the tank geometry, wall characteristics, and overall design. In this study, the gravimetric performance of the cryogenic hydrogen tank and the associated conditioning system are represented with two metrics [Mukhopadhaya et al., 2022], described with equations B1 and B2. A value of GI = 0.25 is assumed, accounting for the expected size of the tank and needed auxiliaries. The detailed calculation of H2 fuel mass by the aforementioned framework is used to estimate the mass of the tank and TMS. Liquid H2 tank dimensions are estimated by accounting for wall thickness and tank filling factor, which depends on the way that the LH2 was stored and kept in the tank. For the size of aircraft investigated herein, one single tank of diameter slightly less than of the fuselage is sufficient. The tank is assumed to be installed in the rear part of the aircraft.

$$Mass\ Factor = MI = \frac{Fuel\ mass}{Fuel\ mass + Tank\ mass}, eq.B1$$

$$Gravimetric\ Index = GI = \\ = \frac{Fuel\ mass}{Fuel\ mass + Tank\ mass + Thermal\ management\ system\ mass}, eq.B2$$

The analysis that follows compares the H2 engine and aircraft with the conventional Jet-A burning one. A design space is generated by varying the engine OPR and COT at cruise, which define the engine cycle. Fuselage length is expected to increase given the addition of the cryogenic H2 tank. **Figure B1** (left) shows the estimated change with respect to the Jet-A case of OPR 13 and COT of 1400 K. An average increase of 7% is found for the design space. The added dry mass from the complete H2 system, including the tank and thermal management system, is normalized with the MTOW of the Jet-A aircraft for OPR 13 and COT 1400 K. A 10% increase in aircraft mass is expected due to the inclusion of the H2 system. This increase does not account for the reduction of fuel given the difference of energy content, which is explored and discussed in the following sections. Increase cycle temperature and pressure ratio lead to less fuel consuming engines, which in turn require less tank and TMS volume and mass.

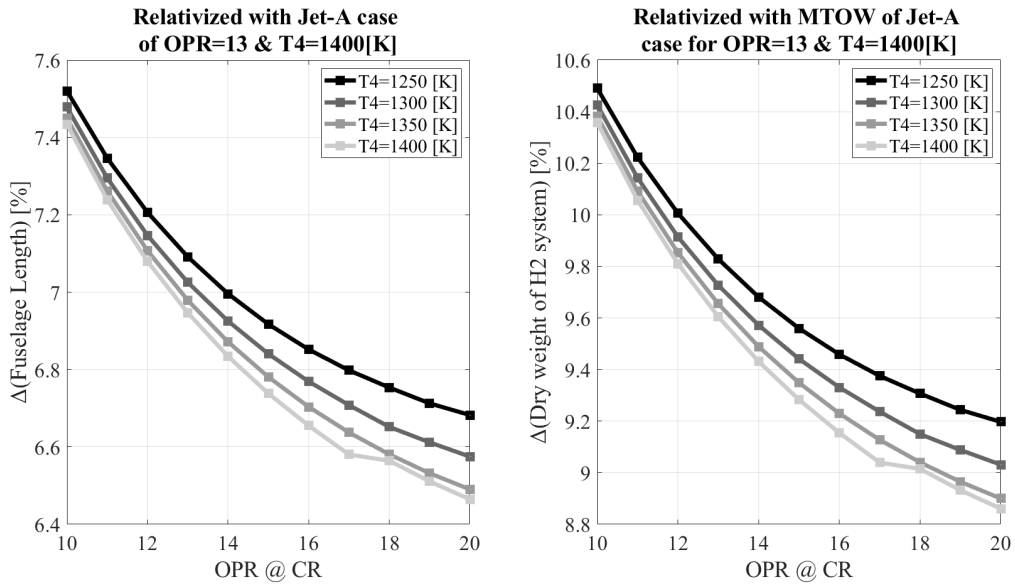

Figure B1. Added length and mass due to H2 system installation.

Finally, the separate and combined impact of the fuselage elongation and added dry H2 system mass on cruise SFC, block fuel and MTOW with respect to the case that only accounts for the change of the engine fuel is reported in **Table B1**. Cruise SFC is improved by the addition of the tank and TMS mass given that the thrust requirement is increased without pushing engine operation in a less efficient region. However, block fuel and MTOW increase significantly, showcasing the importance of accounting for all aspects of H2 integration in the study.

Table B1. Mean impact of hydrogen integration in aircraft performance.

	Mean Impact [%] (difference from the solely burning H2 case)		
Level of H2 integration	**Cruise SFC**	**Block fuel**	**MTOW**
Fuselage elongation	-0.64	1.95	2.55
Fuselage elongation & Added mass for H2 system	-1.96	6.39	15.84

B.2 Results

The analysis that follows compares the H2 configuration, meaning an engine that burns H2 directly and has increased fuselage length and mass due to the complete H2 fuel system. The design space is represented by a variation of cruise OPR between 10 and 20 with an increment of 1, and T4 between 1250 K and 1400 K with an increment of 50 K. Comparisons and relative differences are given in two different ways. H2 engine and aircraft designs are compared with the Jet-A case of OPR 13 and T4 1400K, which acts as the reference conventional design, or they are compared with the Jet-A case of equal OPR and T4. The first way of comparing shows the cumulative effect of fuel change and cycle design variation, while the second way isolates the impact of fuel change by hiding the effect of OPR and T4 variation.

The gas generator of the turboprop engine comprises a high-pressure compressor, combustor, high pressure turbine, free power turbine, and several miscellaneous components, such as shafts, nozzles, ducts, accessories, and bearings. Cruise OPR is varied and T4 remains constant at 1400 K for **Figure B2**. The Jet-A engine is analysed on the left graph and the H2 one on the right. Increased OPR leads to smaller GG mass. It shown that mass contribution from different components remains relatively constant between the Jet-A and H2 configuration. Compared to the Jet-A engine, GGC mass reduces by an average of 8%, GGT mass reduces by an average of 15%, and FPT reduces by an average of 9%.

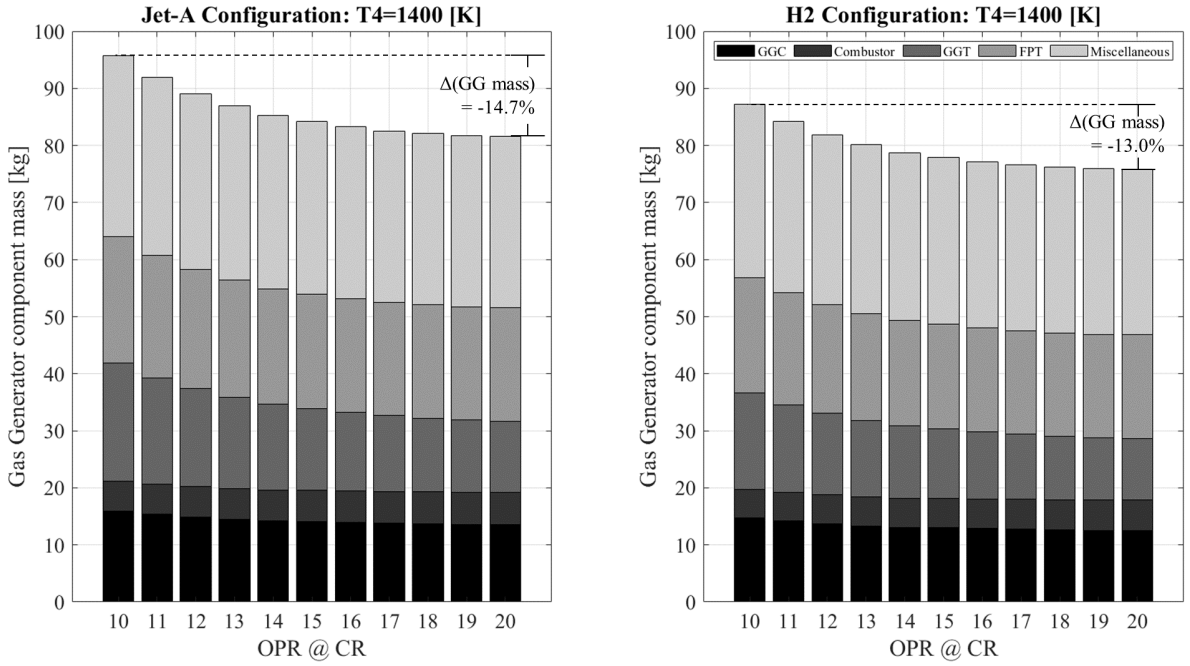

Figure B2. Gas generator component mass breakdown for Jet-A and H2 cases of T4 1400K.

The whole turboprop engine comprises the gas generator, propeller, and propeller gearbox. The two latter components do have any mass variation between the configurations, given that power loading, power requirements, and tip speed limits stay fixed throughout the study. Therefore, a relative GG mass reduction of about 10% for the H2 designs, corresponds to a roughly 3% reduction in terms of whole engine mass. This is indicated in the right graph of **Figure B3**, where the impact of cycle design is obscured by the relativization approach. It is shown that the benefits of whole engine mass reduction are reducing for increased cycle overall pressure ratio and temperature. The left graph, also highlights the importance of COT and OPR, given that mass reduction benefits are achieved only for the hotter and higher-pressure cycle H2 designs.

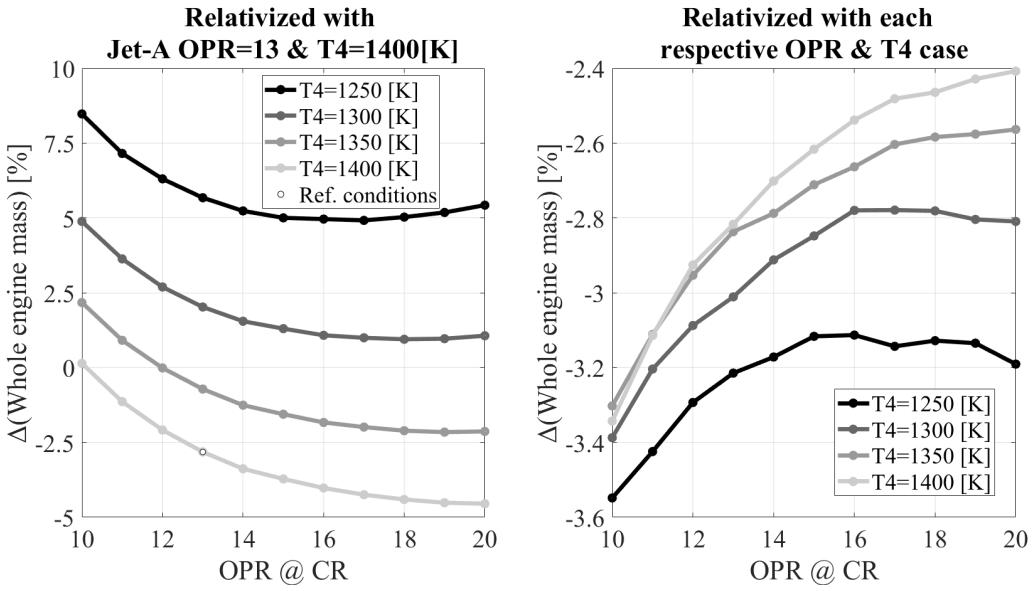

Figure B3. Relative change of whole engine mass.

The relative change of mass flow through the engine components is shown in **Figure B4**. The impact of cycle variation is obscured and only the effect of changing from Jet-A to H2 is shown. H2 combustion

products have higher specific heat capacity and gamma value compared to Jet-A combustion products, therefore, for a given temperature difference less mass flow is required to produce the same amount of work and power. For the FPT, an average relative increase of 4% for the specific heat capacity is calculated. Along with the effect of gamma on temperature and pressure ratios, an average of 5-7% decrease of mass flow is observed through the H2 gas generator.

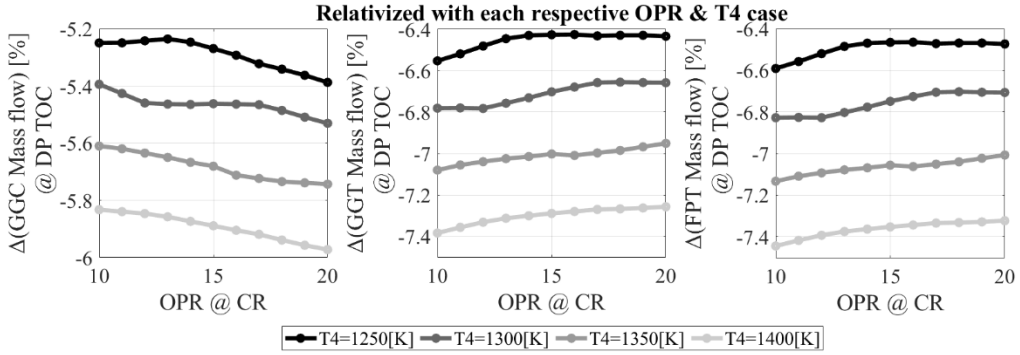

Figure B4. Relative change of mass flow through engine components.

An important aspect of all axial engines of relatively small aircraft and small power settings is the design of the high-pressure compressor, and especially the height of the last blade. The engines of this study that operate under high cycle temperature and pressure have unreasonably small last blades, which are unfeasible with current manufacturing processes. A very optimistic margin at 6mm is chosen for EIS engines of 2035, according to literature [HECARRUS project, 2022]. Yet, it is noted, that the most possible approach for the design of such a compressor would be to take-off the last few stages and replace them with a centrifugal compressor.

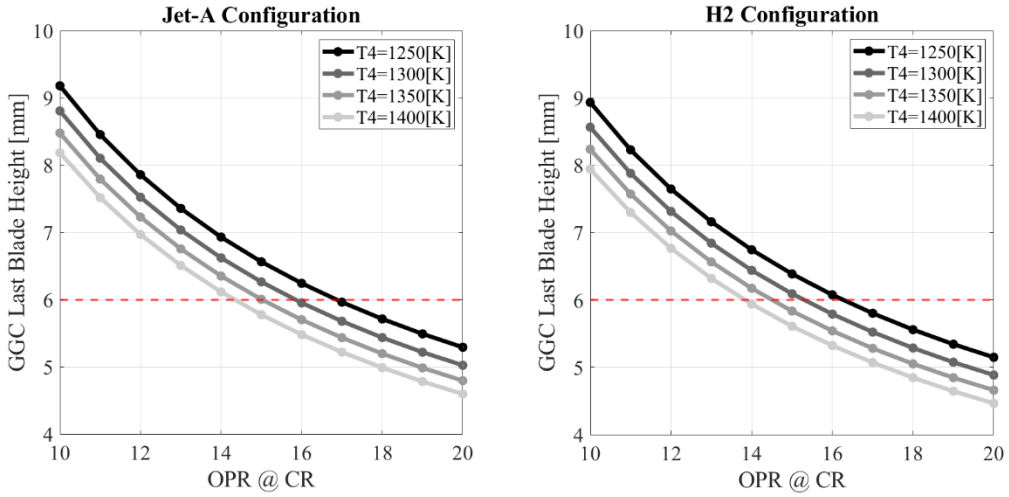

Figure B5. Compressor last blade height for Jet-A and H2 engines.

Kyprianidis et al. [Kyprianidis et al., 2015] derived a correction for the compressor efficiency of engines, according to their last blade height. The correction is translated to an SFC penalty, respective increase in block fuel consumption and also an increase of MTOW. For the results following, this penalty has not been applied but the expected relative values for the cruise OPR range and T4 of 1400K is shown in **Figure B6**. This outcome further fortifies the selection of lower pressure ratios for small engines, despite a first analysis indicating that increasing cruise OPR is always beneficial.

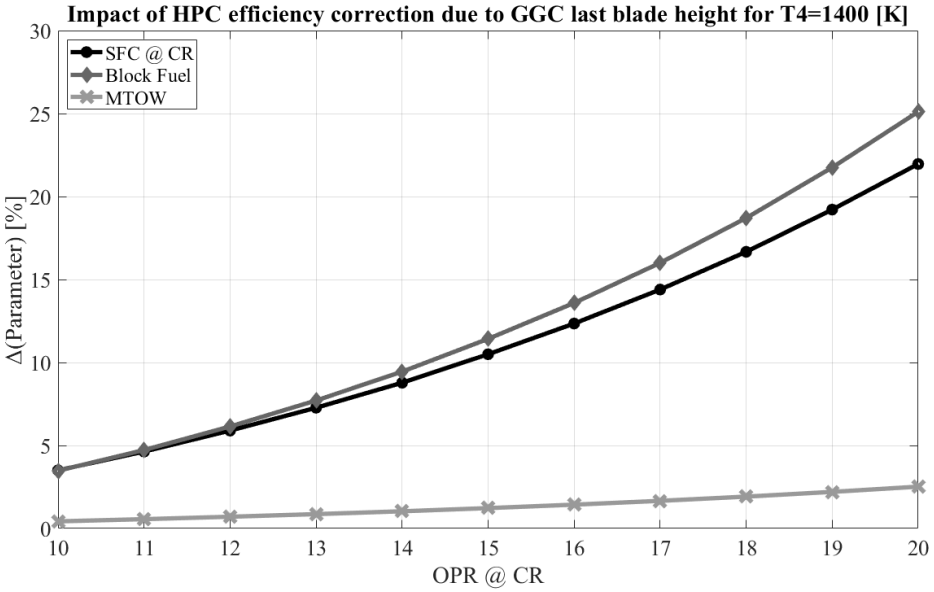

Figure B6. SFC penalty for compressor last blade heights.

Several efficiency definitions are used to describe the engine performance [HECARRUS project, 2022]. Core efficiency shows an improvement of about 1% for the H2 engine, as an effect of the improved specific heat capacity and gamma value. Transfer, installation, and propulsive efficiency do not vary significantly to impact the cumulative outcome that is observed for the overall efficiency of the H2 engine, which improves in the range of 0.6-0.8% for the examined OPR range and T4 of 1400K. Finaly, thermal efficiency, also shows an improvement in the same scale stemming from the change of fuels and corresponding impact on fluid properties of combustion products. Values of **Table B3** refer to absolute change of efficiencies.

Table B3. Impact of H2 burning on engine efficiencies.

	OPR=13 & T4=1400 [K]	**Varying OPR and T4=1400 [K]**
	Δ(efficiency) [%]	**Range of Δ(efficiency) [%]**
Core efficiency	0.92	[0.85 - 1.05]
Overall efficiency	0.68	[0.63 - 0.78]
Thermal efficiency	0.79	[0.73 - 0.90]

The equivalent specific fuel consumption is a metric used to equate the fuel consumption of the H2 and Jet-A engines by normalizing the impact of the fuel's energy density. The definition is given in equation B3.

$$ESFC = \frac{SFC_{H2}}{LHV_{Jet-A}} * LHV_{H2}, eq.B3$$

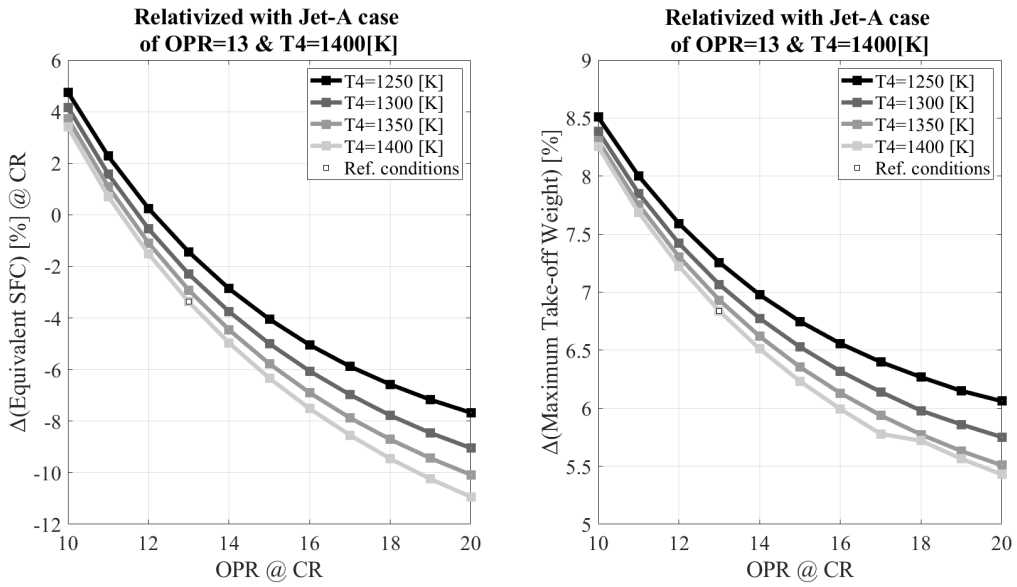

Figure B7. Change in equivalent specific fuel consumption at cruise and maximum take-off weight for H2 configuration compared to reference Jet-A case.

The left graph of **Figure B7** presents the relative change in ESFC at cruise for the H2 configurations with respect to the SFC of the reference Jet-A case. For the reference conditions, the impact of cycle design variation does not effect the relative change, therefore, the 3.5% reduction in specific fuel consumption for OPR 13 and T4 1400K corresponds solely to the effect of changing from Jet-A to H2. The improvements in engine performance and higher thrust requirement lead to the improvement of SFC for the H2 aircraft. However, at the same graph the impact of increasing OPR and T4 can also be observed. An increase of OPR by 1, until reasonable OPR values results in a further 2% reduction of SFC, which is comparable to the impact that changing fuels presents. The impact of increasing T4 to improve SFC is more pronounced for larger OPR values and leads to a further 1% decrease at most. The right graph of Figure B7 indicates the relative change of the H2 aircraft compared to the reference Jet-A case. The change of fuels leads to an increase in MTOW of about 7%. The impact of cycle design on MTOW is comparable to change of fuel but about 3 times less for the examined design space.

The variation in equivalent specific fuel consumption which stems from the slightly improved performance of the H2 engine, and the aircraft added weight due to the H2 fuel system are the two competing factors that determine the overall energy consumption of the H2 aircraft. The relative change in block energy requirements is presented in **Figure B8**. The left graph is relativized with the reference case, and the right one is relativized with each respective OPR and T4 Jet-A case. Not accounting for the impact of cycle design, an average of 1.5% increase in block energy requirements is observed for the H2 configurations. This is strongly dependent on the added H2 system mass and therefore the selection of the gravimetric index. It is noted, however, that a gravimetric index of 0.25 leads to almost equal energy demands for the H2 and Jet-A configurations. The left graph of Figure B8, also shows the effect that OPR and T4 have on the energy requirements of the configurations. An increase of OPR by 1 has equal impact with the change of fuels in the configuration.

It is noted that despite the energy requirement being about equal, the H2 configuration results in zero CO2 emissions, while the reference Jet-A case emits about 1.3 tones of CO2 during the main mission.

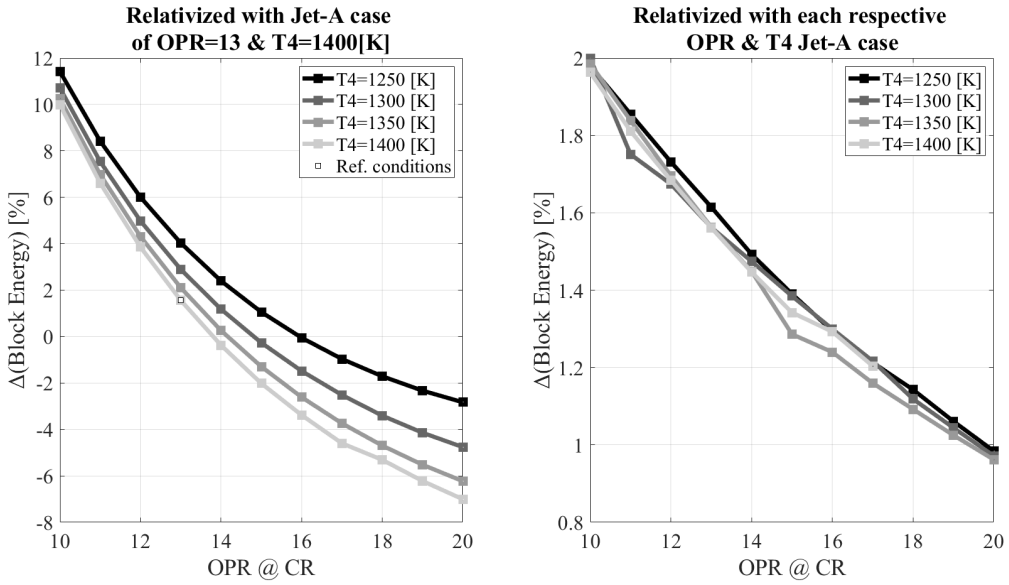

Figure B8. Change in block energy consumption for H2 configuration compared to Jet-A cases.

C. Ground infrastructure

A system-level simulation and optimization framework for airports serving as energy hubs for hybrid electric and hydrogen powered aviation is developed. The framework comprises linear models for the individual components of the system, namely:

- External supply of compressed and liquid hydrogen, through trucks and/or a pipe network.
- Storage tanks for compressed and liquid hydrogen, including compression and liquification units.
- A proton exchange membrane (PEM) electrolyzer for converting electricity into hydrogen.
- A PEM fuel cell for converting hydrogen into electricity.
- A lithium-ion (Li-ion) battery system for storing electricity.
- A system of ground/roof photovoltaic (PV) panels for renewable electricity generated on site.
- A simplified model for supply of electricity from and to the regional power grid.
- A simplified model of the demand for liquid and compressed hydrogen by the aircraft, as well as ground vehicles in the vicinity of the airport.
- A simplified model for electricity demand by the aircraft, ground vehicles and ground systems within or adjacent to the airport terminals.

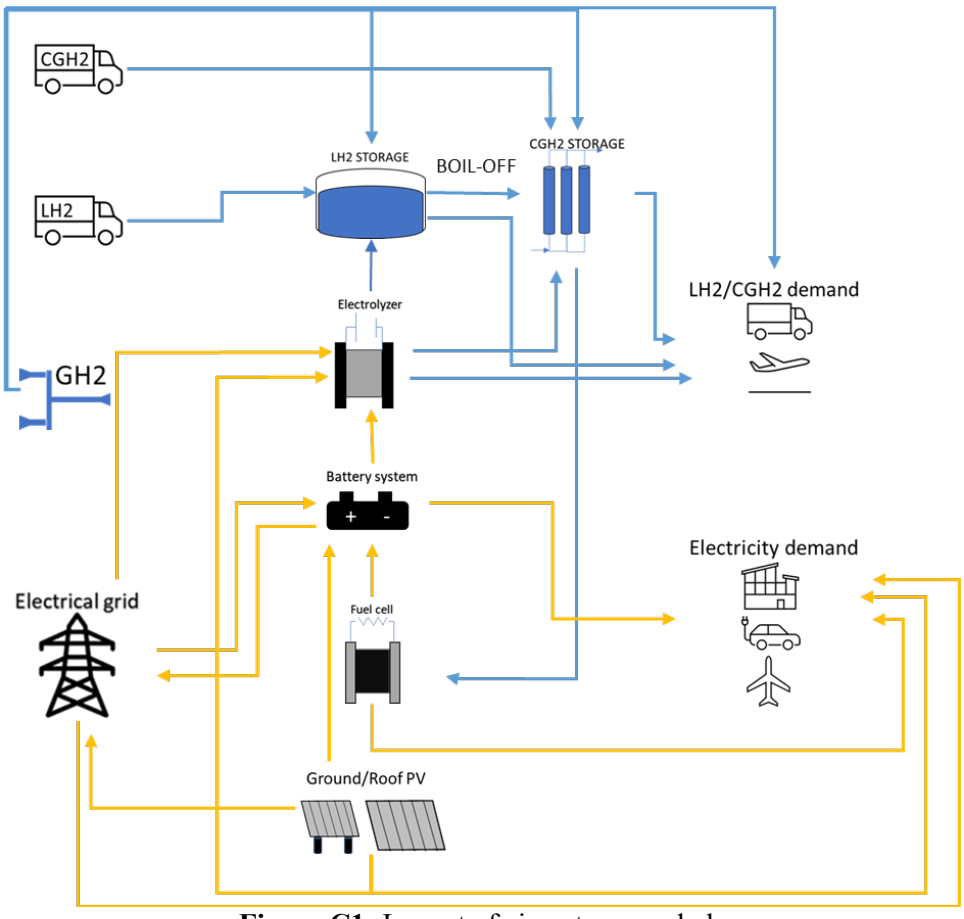

Figure C1: Layout of airport energy hub

The integrated system along with the corresponding interconnections between the components is illustrated in **Fig. C1**. Representative efficiencies and specifications have been selected for each component based on literature suggestions and market values, considering technology maturity levels of 2035. Interconnections between the individual components represent bilateral flow of energy in different forms, enabling multiple possibilities for the flexible operation of the hybrid system, in

connection to the main power grid. For example, the battery system can store electricity produced by the fuel cell, but also provide electricity to the electrolyzer, or exchange with the grid, or even supply the electrified aircraft or ground vehicles.

The major parameters that form the boundary conditions to the system operation are:

- Market factors such as electricity or hydrogen prices
- Volatility in own production of electricity through solar panels
- Demand in electricity and hydrogen by the airborne and ground consumers

Historical data is employed for representing electricity price variations, referring to a selected week in December 2023 (1 December to 7 December) within the SE3 energy region in Sweden. Historical solar irradiance profiles are utilized for the same period. The designated time period has been selected to investigate the operation of the airport hub under conditions of relatively high and volatile electricity prices combined with relatively low levels of solar irradiance for own production of electricity. A realistic price has been considered for externally supplied compressed and liquid hydrogen, assuming that it is produced by renewable electricity. The accrued distributions for electricity price, solar irradiance, and hydrogen prices are illustrated in **Fig. C2**.

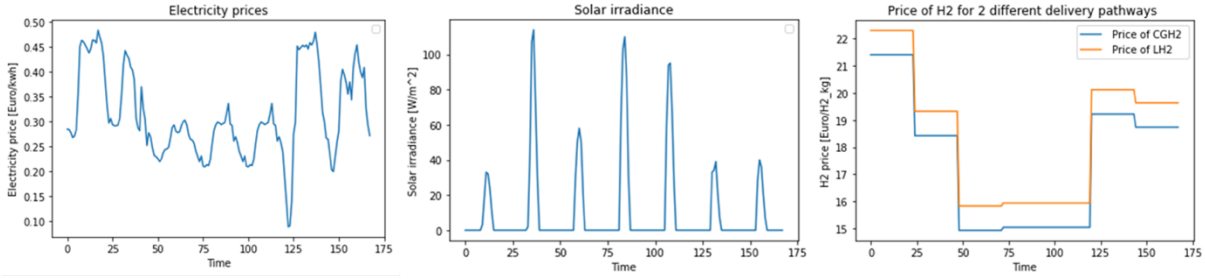

Figure C2: Time distributions for electricity price, solar irradiance, and hydrogen prices employed in the optimization campaign.

A representative flight schedule was constructed based on public data, conservative extrapolations, and engineering judgement. The regional airport in the city of Västerås (Stockholm Västerås Airport – VST) was considered as a presently small airport with potential for developing into a hub for electrified and hydrogen powered regional aviation. Västerås constitutes an established and rapidly growing hub for industrial electrification in Sweden, therefore, investigations on a potentially electrified airport connected to the power grid is of great relevance and importance.

An assumed future aircraft fleet mix is considered for the 2035 timeframe, comprising hydrd electric aircraft of low degree of hybridization (20%) along with hydrogen powered aircraft and conventionally fueled aircraft. An approximation to annual electricity demand for the operation of the terminals, shops, runway areas and parking lots was derived out public data from Stockholm Arlanda Airport, downscaled to Stockholm Västerås Airport. The obtained profile of scheduled flights per hour for the selected period of one week is represented in **Fig. C3**.

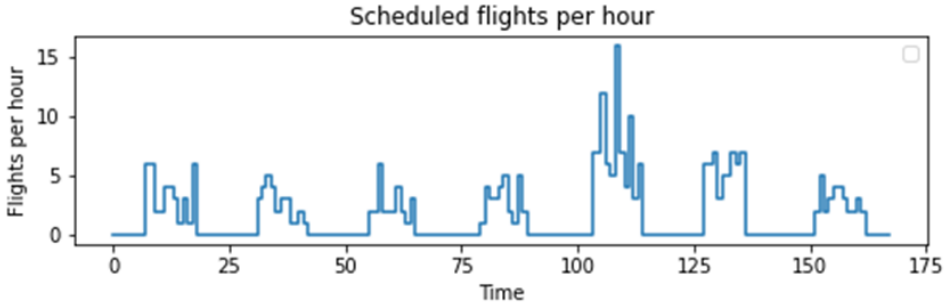

Figure C3: Distribution of scheduled flight per hour at Västerås airport in the 2035 timeframe

The corresponding demands for electricity and hydrogen to power the scheduled flights are illustrated in **Fig. C4** and **Fig. C5**, respectively. It is noted that the selected window of one week is considered as representative period to capture typical periodical activity patterns within an airport.

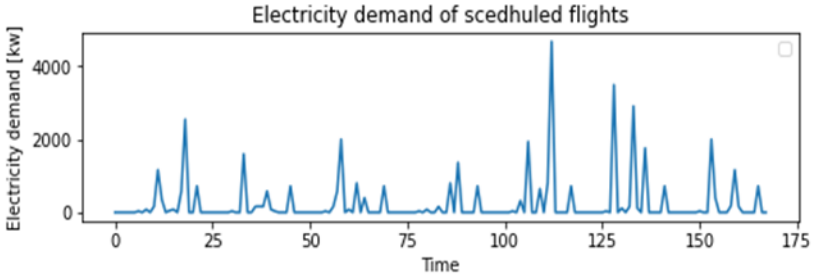

Figure C4: Electricity demand profile for scheduled flights at Västerås Airport in 2035

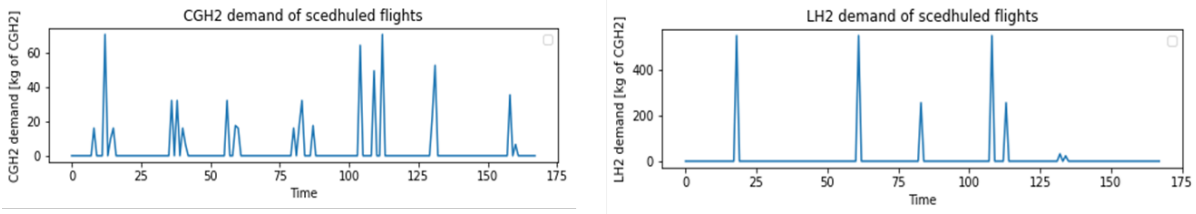

Figure C5: Compressed and liquid hydrogen demand profiles for scheduled flights at Västerås Airport in 2035

Electricity demand to cover the power needs for the terminals and ground infrastructure is presented in **Fig. C6**. It is observed that ground electricity demands are considerably lower than the ones of the electrified aircraft, nevertheless they contribute to the combined electricity demand profile, as shown in **Fig. C7**.

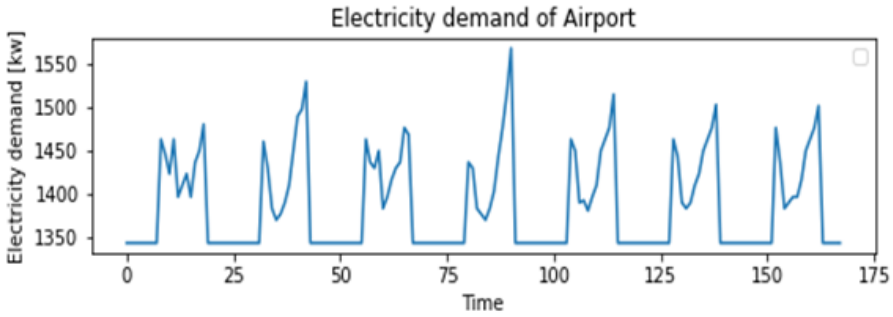

Figure C6: Electricity demand profiles for terminals and ground infrastructure at Västerås Airport in 2035.

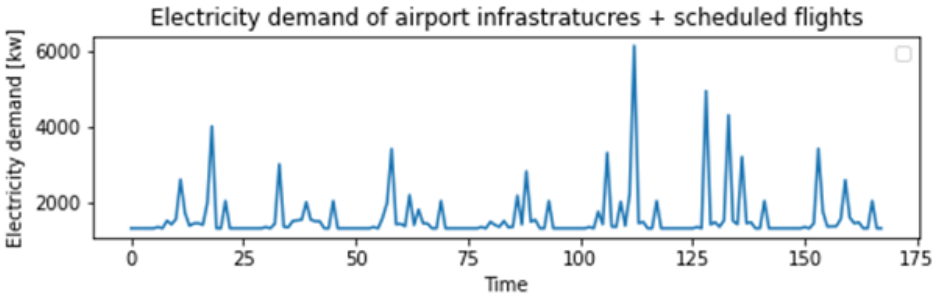

Figure C7: Overall electricity demand profile for airborne and ground consumers at Västerås Airport in 2035.

An operational optimization strategy is established aiming at minimizing the overall operational cost for the system. Operational parameters for the airport energy system components, together with the corresponding interconnections among them, yield a total number of 30 continuous decision variables in the hands of operators and planners. Additionally, a total of 8 binary (on/off) decision variables render a complex multi-variable optimization problem under volatile inputs and external disturbances. Furthermore, a set of operational and design constraints is considered for each and every component of the system, referring to maximum and minimum capacities for the storage components, charge and discharge rates according to market recommended values, rated power for the electrochemical conversion devices, as well as practical limitations on external supplies of hydrogen and electricity.

The objective of the complex optimization problem is to minimize the total operating cost along the examined period, on an hourly time resolution. The major cost components are listed below:

- External supply of electricity from the grid
- External supply of liquid and compressed hydrogen
- Cost of internal compression and liquification of hydrogen
- Cost for production of liquid and compressed hydrogen

The optimized distribution of electricity streams in the examined period is presented in **Fig. C8**. It is observed that own production of electricity from the PV panels is marginal, due to the low solar irradiance levels in the month of December in Sweden. Therefore, the airport relies on the power grid for covering a substantial amount of the base demand of electricity. However, it is observed that the battery system covers the complete electrical load during instances of high demand combined with high electricity prices. Therefore, the optimizer takes advantage of low electricity prices to cover running demands and charge the batteries at the same time, whilst decouples from the grid when the cost for purchasing electricity is high. Particularly for the period where electricity prices encompass a significantly low peak (i.e. around Time=120h), enough hydrogen surplus is produced so that it is fed to the fuel cell for additional electricity production. The battery charging profiles demonstrate that the battery system is predominantly charged by the grid due to the low production from the PV panels. Charging takes place during periods of lower electricity price. Subsequently, the airport energy hub sells electricity to the grid when electricity price is higher through discharging the batteries.

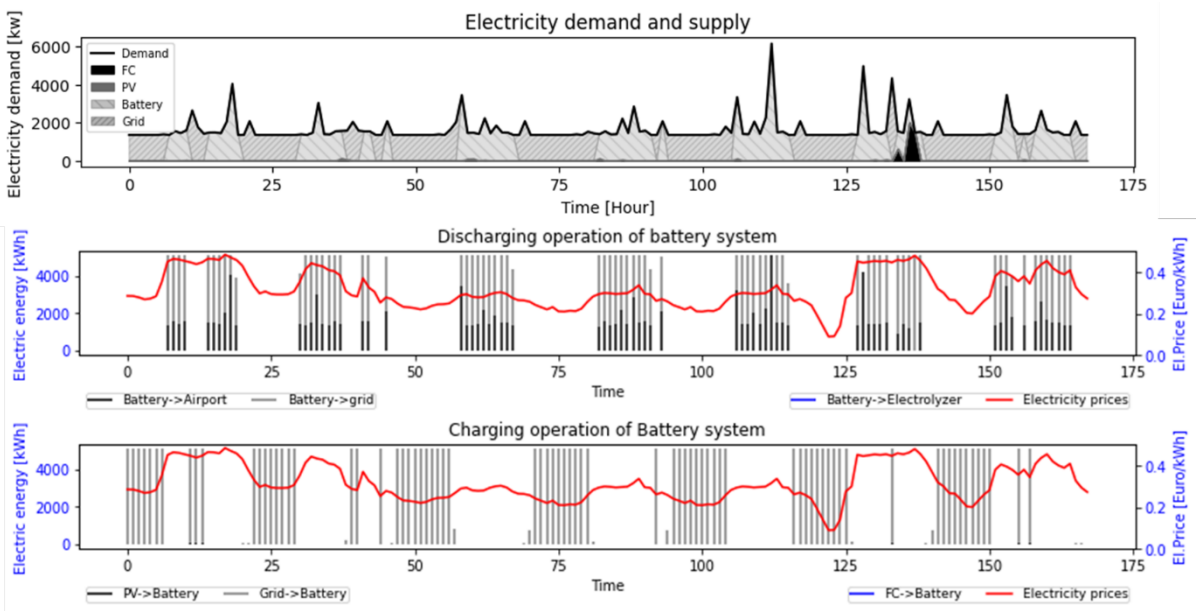

Figure C8: Optimal operation for electricity stream and corresponding battery storage unit.

The optimized energy streams for compressed hydrogen are presented in **Fig. C9**. The demand for compressed hydrogen is primarily met through first storing it into the gas tank, whilst at rare instances, hydrogen is supplied to the airport consumers directly through the electrolyzer without prior storage. It is noted that the gas tank is supplied with compressed hydrogen by both own production through the electrolyzer and external supply. Own production is preferred when the corresponding cost is lower than the cost of external purchase of hydrogen. A part of the compressed hydrogen, instead of directly using it in a fuel cell or the ground or air vehicles, it is converted into liquid for use in liquid hydrogen powered aircraft.

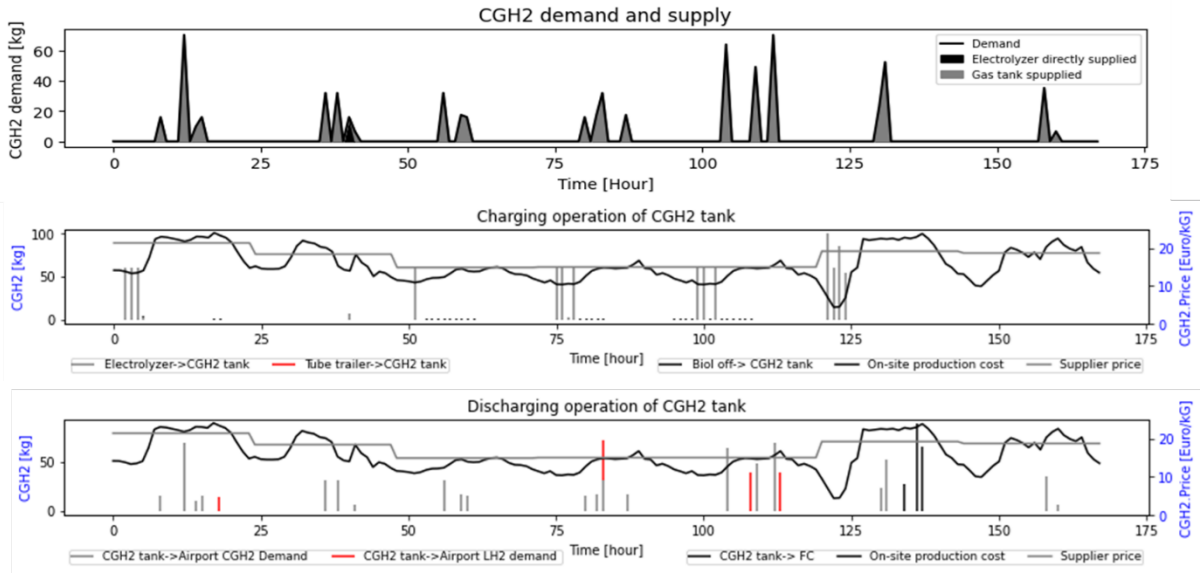

Figure C9: Optimal operation for compressed hydrogen stream and corresponding storage unit.

The optimized energy streams for liquid hydrogen are presented in **Fig. C10**. Liquid hydrogen is exclusively used by hydrogen-burning aircraft and is predominantly provided by liquid storage tanks. Liquid hydrogen is either produced on site or supplied to the airport by trucks. No export of liquid hydrogen from the airport to the energy grid is considered. It is shown that the cost for own production is often lower than the cost of external supply of liquid hydrogen which is something to be considered in future investments in airport infrastructure.

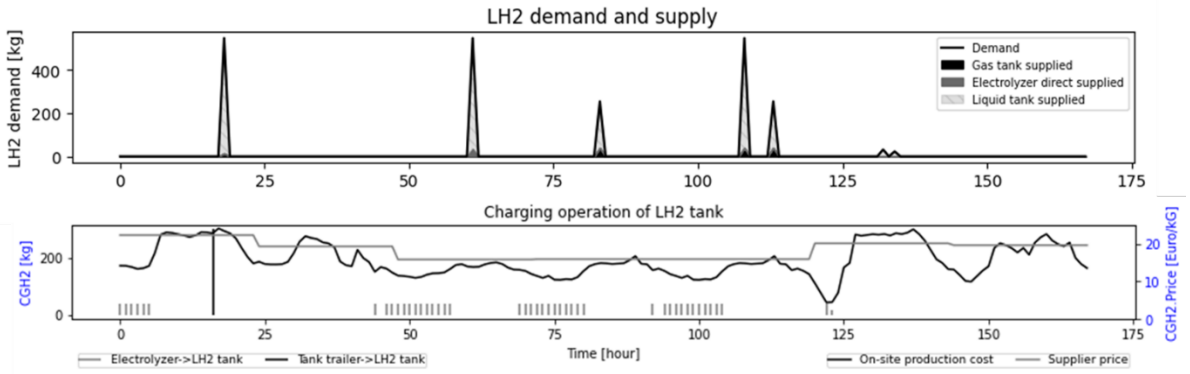

Figure C10: Optimized operation for liquid hydrogen stream and corresponding storage unit.

A detailed study on the cost of hydrogen production in the vicinity of Swedish regional airports is carried out. Stockholm Skavsta airport (NYO) is selected for this investigation. A similar to

the above-described system is considered for electricity flows, i.e. own production through solar panels and combined with grid-supplied electricity.

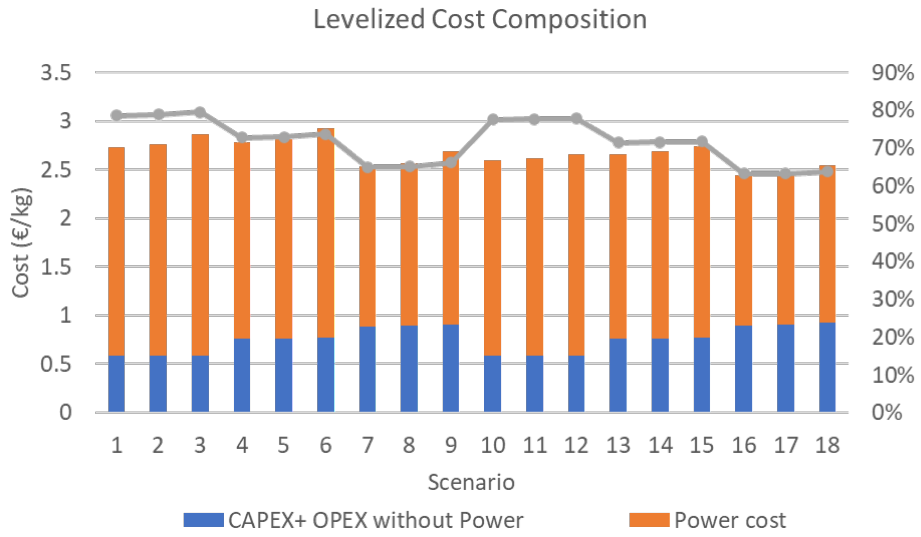

Figure C11: Levelized cost of hydrogen production

The levelized cost of hydrogen production is presented in **Fig. C11**. The cost is broken down into the equivalent capital and operating cost (CAPEX and OPEX) and the cost of actual power generation. It is observed that the cost of power generation corresponds to 65-80% (gray line) of the total cost which showcases the need for technological advancements in component technologies to bring the cost further down.

An additional detailed study on the supply cost for hydrogen is carried out. A dedicated offshore wind power farm is considered in the Norrtälje area, developed to provide Stockholm Arlanda airport (ARN) with hydrogen. Different transportation methods are considered, namely pipeline, ferry transport, and road transport, as shown in **Fig. C12**.

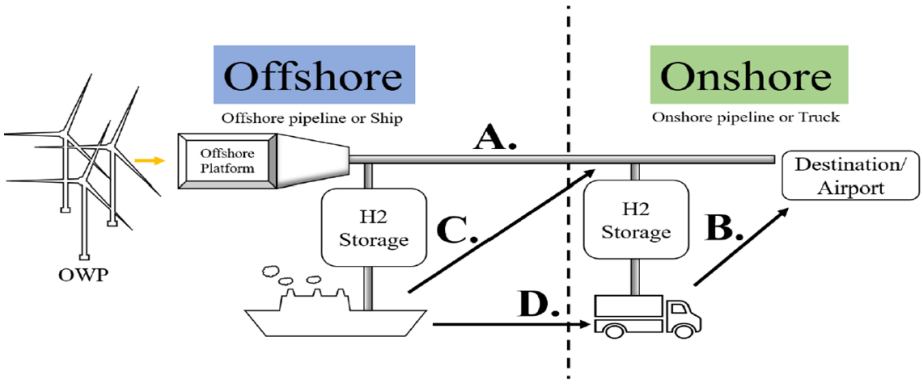

Figure C12: Potential transportation and supply methods for hydrogen

The offshore wind farm is equiped with an electrolyzer to convert electricity into hydrogen. Two types of electrolyzers were considered: PEM Electrolyzer (PEMEL), same as in the previous studies and alkaline electrolyzer (AEL) as an alternative. The levelized cost of transporting hydrogen as function of distance is presented in **Fig. C13**.

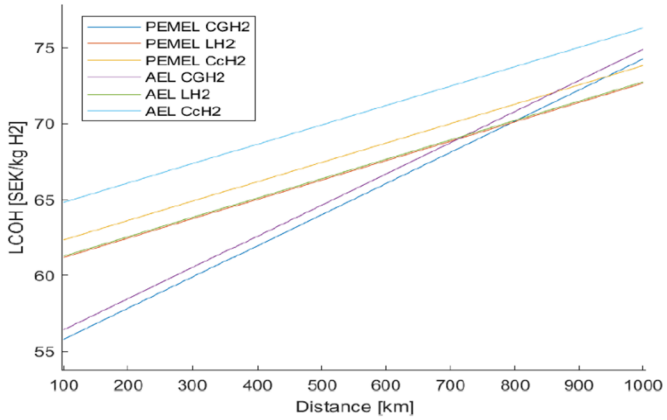

Figure C13: Levelized cost of transporting hydrogen to the airport, as function of distance.

It is observed that the distance between between the production site and the airport is of decisive importance for the economic viability of different conversion scenarios. For example, for the case of PEM electrolyzer and compressed hydrogen, doubling the distance from 500 to 1000 km yields a 15% increase in the levelized cost of transportation. This is a direction for future energy infrastructure developments and the strategic decision of newly built renewable energy power plants.

Discussion

Investigation of the hybrid-electric aircraft revealed that there are several underlying interdependences between the electrical and thermal powerplant. A two-way influence between turbomachinery and electrical power system design points on the integrated power system is revealed. An opposing trend between electrical and conventional powertrain mass is driven by electric fan design power. Power system efficiency improvements in the order of 2% favor high-power electric fan designs. A trade-off in electrical power system mass and performance arises from oversizing of electrical components for load manipulation. Branch efficiency improvements of up to 3% imply potential to achieve battery mass reduction due to fewer transmission losses. A threshold system voltage of 1kV, yielding 32% mass reduction of electrical branches and performance improvements of 1-2%, is identified. The analysis sets the foundation for interpreting mission-level electrification outcomes that are driven by interactions on the integrated power system. Areas of conflicting interests and synergistic opportunities are highlighted for optimal conceptual design of hybrid powertrains.

The aircraft and mission performance investigation revealed that the reference designed hybrid-electric configuration with entry-into-service 2035 assumed technologies yields roughly 18% improvement in block consumption and emissions, but an 8% increase in maximum take-off weight, compared to its 2014 conventional counterpart. The design space exploration for an optimal power management scheme indicated a minimum average ratio of 1:1.35 between cruise and design point hybridization power. Despite this area not being the optimal in terms of individual power system performance, full depletion of the installed electrical energy yields best results in that region. Potential of further electrification increase is feasible if the initial top-level aircraft constraints are slightly relaxed. Heavier and more electrified designs results in further consumption and emissions improvements in the order of 5%, with battery systems of up to 1300 kg.

Hydrogen propulsion is also investigated for its potential to alleviate the environmental impact of aviation. Direct hydrogen combustion and storage in cryogenic tanks is explored. Given the energy density of H2, the carried fuel reduces significantly. However, the aircraft increases compared to the conventional configuration due to the added mass of the H2 tank and thermal conditioning system. Direct combustion of H2 results to the design of slightly more efficient gas turbines due to the increase of specific heat capacity. This also leads to smaller engines. The improved performance and reduced carried fuel compete with the increase mass of the complete fuel system, results in an overall penalty in block energy requirements compared to the conventional configuration.

Development of ground infrastructure in the vicinity of airports is essential for the implementation of electrified and hydrogen powered flight. A regional airport shall not exclusively rely on the grid but rather develop infrastructure for own production of renewable electricity and green hydrogen, compressed and liquid. The capacity for external supply of electricity from the power grid to the airport determines the necessary size for the infrastructure investment. At the same time, it depicts the need for upscaling in renewable-based electricity generation by the power grid to enable the transition to fossil-fuel free aviation. Concurrently, own production of electricity and hydrogen in the premised of the airport de-risks from supply-chain-related issues, and quite often, provides a lower cost compared to external purchase. At the same time, the airport can contribute to the power grid through selling surplus electricity. Overall, the role of an airport energy hub is to create the link between fossil-free flight and a sustainable power grid, enabling the transition to a greener aviation and energy sector.

Publications list

Bermperis, Dimitrios, Mavroudis D. Kavvalos, Stavros Vouros, Konstantinos G. Kyprianidis. " ADVANCED POWER MANAGEMENT STRATEGIES FOR COMPLEX HYBRID-ELECTRIC AIRCRAFT." In *Turbo Expo: Power for Land, Sea, and Air*, London, United Kingdom, 2024 **(submitted)**.

Bermperis, Dimitrios, and Kyprianidis, Konstantinos. "Comparative Design of Hydrogen-Fired and Electrified Turboshaft for Sustainability" In International Symposium on Air Breathing Engines, ISABE 2024, Toulouse, France, 22-27 Sep 2024 **(submitted)**.

Bermperis, Dimitrios, Elissaios Ntouvelos, Mavroudis D. Kavvalos, Stavros Vouros, Konstantinos G. Kyprianidis, and Anestis I. Kalfas. "Synergies and Trade-Offs in Hybrid Propulsion Systems Through Physics-Based Electrical Component Modeling." Journal of Engineering for Gas Turbines and Power 146, no. 1 (2024): 011005.

Taha M., Lundvall N., Kyprianidis K., Salman A., Vouros S., Zaccaria V. “Techno-economic evaluation of hydrogen production for airport hubs”, In the 15th International Conference on Applied Energy, Dec. 2023, Doha, Qatar.

Vouros, S., Hieb, D. and Kyprianidis, K., 2022, June. Impact of Boundary Layer Ingestion on the Performance of Propeller Systems for Hybrid Electric Aircraft. In *Turbo Expo: Power for Land, Sea, and Air* (Vol. 85970, p. V001T01A025). American Society of Mechanical Engineers.

References, sources

Bermperis, Dimitrios, Elissaios Ntouvelos, Mavroudis D. Kavvalos, Stavros Vouros, Konstantinos G. Kyprianidis, and Anestis I. Kalfas. "Synergies and Trade-Offs in Hybrid Propulsion Systems Through Physics-Based Electrical Component Modeling." Journal of Engineering for Gas Turbines and Power 146, no. 1 (2024): 011005.

Bradley, M.K. and Droney, C.K., 2015. Subsonic ultra green aircraft research: Phase 2. Volume 2; Hybrid electric design exploration.

Bradley, T., Moffitt, B., Parekh, D., Fuller, T. and Mavris, D., 2009, August. Energy management for fuel cell powered hybrid-electric aircraft. In 7th international energy conversion engineering conference (p. 4590).

Bradley, T.H., Moffitt, B.A., Mavris, D.N. and Parekh, D.E., 2007. Development and experimental characterization of a fuel cell powered aircraft. Journal of Power sources, 171(2), pp.793-801.

Chen, Mi, Rincon-Mora, Gabriel A. Accurate electrical battery model capable of predicting runtime and IV performance. IEEE transactions on energy conversion, 21(2), (2006). pp.504-511. DOI: 10.1109/TEC.2006.874229

Clean Sky 2 JU, Hydrogen-powered aviation | A fact-based study of hydrogen technology, economics, and climate impact by 2050, 2020

DelRosario, R., 2014. A future with hybrid electric propulsion systems: A NASA perspective.

Giannakakis, P., Maldonado, Y.B., Tantot, N., Frantz, C. and Belleville, M., 2019. Fuel burn evaluation of a turbo-electric propulsive fuselage aircraft. In AIAA Propulsion and Energy 2019 Forum (p. 4181).

Guynn, M.D., Freeh, J.E. and Olson, E.D., 2004. Evaluation of Hydrogen Fuel Cell Powered Blended-Wing-Body Aircraft Concept for Reduced Noise and Emissions.

HECARRUS Project. "D2.3: Sizing, layout and performance of critical technologies". 2022

HECARRUS Project. "D3.3: Final report on the preliminary design review of a conceptual hybrid commuter aircraft", 2022.

IATA, 2019. Aircraft Technology Roadmap to 2050

Infineon Technical Documentation. "Dimensioning program IPOSIM for loss and thermal calculation of Infineon IGBT modules". Infineon Technologies.

Jansen, R., Bowman, C., Jankovsky, A., Dyson, R. and Felder, J., 2017. Overview of NASA electrified aircraft propulsion (EAP) research for large subsonic transports. In 53rd AIAA/SAE/ASEE Joint Propulsion Conference (p. 4701).

Jenkinson, Lloyd R., Paul Simpkin, Darren Rhodes, Lloyd R. Jenkison, and Rolls Royce. Civil jet aircraft design. Vol. 338. London: Arnold, 1999.

Kavvalos, Mavroudis, Xin, Zhao, Schnell, Rainer, Aslanidou, Ioanna, Kalfas, Anestis, and Kyprianidis, Konstantinos G. "A Modelling approach of variable geometry for low pressure ratio fans." *In International Symposium on Air Breathing Engines, ISABE 2019*, Canberra, Australia, 23-27 September 2019 Paper No. ISABE-2019-24382. 2019.

Kim, T. and Kwon, S., 2012. Design and development of a fuel cell-powered small unmanned aircraft. International Journal of Hydrogen Energy, 37(1), pp.615-622.

Kyprianidis, Konstantinos. "An approach to multi-disciplinary aero engine conceptual design." In International Symposium on Air Breathing Engines, ISABE 2017, Manchester, United Kingdom, 3-8 September 2017 Paper No. ISABE-2017-22661. 2017.

Laskaris, Konstantinos. "Design and manufacturing of permanent magnet motors for electric vehicles." PhD Thesis. National Technical University of Athens (NTUA). 2011.

Magnussen, Freddy. "On design and analysis of synchronous permanent magnet machines for field-weakening operation in hybrid electric vehicles." PhD Thesis. KTH Royal Institute of Technology. 2004.

Martínez, Daniel. "Design of a permanent-magnet synchronous machine with non-overlapping concentrated windings for the shell eco marathon urban prototype." Master's Thesis. KTH Royal Institute of Technology (2012).

Mukhopadhaya, Jayant, and Dan Rutherford. "Performance analysis of evolutionary hydrogen-powered aircraft." *ICCT white paper* (2022).

National Fire Protection Association, National electrical code – NFPA 70. Vol. 70. 2014.

Pornet C, Kaiser S, Isikveren AT, Hornung M. Integrated fuel-battery hybrid for a narrow-body sized transport aircraft. Aircraft Engineering and Aerospace Technology: An International Journal. 2014 Sep 30.

Rao, Dantam K. and Kuptsov, Vladimir. "Effective use of magnetization data in the design of electric machines with overfluxed regions." IEEE Transactions on Magnetics 51, no. 7 (2015): 1-9. Doi: 10.1109/TMAG.2015.2397398

Roskam, J., 1985. Airplane design. DARcorporation

Sadey, David J., Csank, Jeffrey, Hanlon, Patrick A. and Jansen, Ralph. "A generalized power system architecture sizing and analysis framework." *In 2018 Joint Propulsion Conference*, AIAA 2018-4616. p. 4616. July 9-11, 2018. Cincinnati, OH, USA. Doi: https://doi.org/10.2514/6.2018-4616

Sielemann, Michael, Kavvalos, Mavroudis D., Selvan, Nithish, Claesson, Jim and Kyprianidis, Konstantinos G. "Select Trade-Offs in Parallel Hybrid Turboprop Cycle Design." *Proceedings of the ASME Turbo Expo 2022: Turbomachinery Technical Conference and Exposition. Volume 1: Aircraft Engine; Ceramics and Ceramic Composites*. Rotterdam, Netherlands. June 13–17, 2022. V001T01A014. ASME. https://doi.org/ 10.1115/GT2022-81629

Srinath, Akshay Nag, Álvaro Pena López, Seyed Alireza Miran Fashandi, Sylvain Lechat, Giampiero di Legge, Seyed Ali Nabavi, Theoklis Nikolaidis, and Soheil Jafari. "Thermal management system architecture for hydrogen-powered propulsion technologies: Practices, thematic clusters, system architectures, future challenges, and opportunities." *Energies* 15, no. 1 (2022): 304.

Tong, Michael T. and Naylor, Bret A. "An object-oriented computer code for aircraft engine weight estimation." *In Turbo Expo: Power for Land, Sea, and Air*, vol. 43116, GT2008-50062. pp. 1-7. June 9-13, 2008. Berlin, Germany. Doi: https://doi.org/10.1115/GT2008-50062

Torenbeek, Egbert. Synthesis of subsonic airplane design: an introduction to the preliminary design of subsonic general aviation and transport aircraft, with emphasis on layout, aerodynamic design, propulsion and performance. Springer Science & Business Media, 2013.

Verstraete, D., 2013. Long range transport aircraft using hydrogen fuel. International journal of hydrogen energy, 38(34), pp.14824-14831.

Vouros S., Kavvalos M.D., Sahoo S. and Kyprianidis K.G., 2020, Enabling the Potential of Hyrbid Electric Propulsion through Lean-Burn-Combustion Turbofans, In Global Power and Propulsion Society Forum 2020

Vratny, Patrick Christoph. "Conceptual design methods of electric power architectures for hybrid energy aircraft." PhD Thesis. Technische Universität München, 2019

Winnefeld, Christopher, Thomas Kadyk, Boris Bensmann, Ulrike Krewer, and Richard Hanke-Rauschenbach. "Modelling and designing cryogenic hydrogen tanks for future aircraft applications." *Energies* 11, no. 1 (2018): 105.

Woolmer, Tim J. and McCulloch, Malcom D. "Axial flux permanent magnet machines: A new topology for high performance applications." IET – The institution of Engineering and technology hybrid Vehicle conference. December 12-13, 2006. Coverty, UK.

Yılmaz, İ., İlbaş, M., Taştan, M. and Tarhan, C., 2012. Investigation of hydrogen usage in aviation industry. Energy conversion and management, 63, pp.63-69.

Zhao, X., Sahoo, S., Kyprianidis, K., Rantzer, J. and Sielemann, M., 2019. Off-design performance analysis of hybridised aircraft gas turbine. The Aeronautical Journal, 123(1270), pp.1999-2018.

Zhao, X., Sahoo, S., Kyprianidis, K., Sumsurooah, S., Valente, G., Rashed, M., Vakil, G., Hill, C.I., Jacob, C., Gobbin, A. and Bardenhagen, A., 2019, June. A framework for optimization of hybrid aircraft. In ASME Turbo Expo 2019: Turbomachinery Technical Conference and Exposition. American Society of Mechanical Engineers Digital Collection.

Attachments

Administrativ bilaga.